Summer 1971

Observations on the Hydraulic Regime of the Ridge and Swale Topography of the Inner Virginia Shelf

Barry W. Holliday
Old Dominion University

OBSERVATIONS ON THE HYDRAULIC REGIME OF THE RIDGE AND SWALE TOPOGRAPHY OF THE INNER VIRGINIA SHELF

by

Barry W. Holliday

A THESIS

submitted to the Institute of Oceanography
Old Dominion University, Norfolk, Virginia
in partial fulfillment of the requirements
for the degree of

Master of Science

August 1971

Committee

Chairman Donald Swift

Ronald E. Johnson

Robert Cheng

ABSTRACT

The Virginia inner shelf is dominated by southwest-trending sand ridges. Wavelengths are 2 to 4 km; amplitudes are up to 10 m; crests can be traced for up to 10 cm. Nearshore ridges trend southwest into the shore face and merge with it at depths as shoal as 5 m. The ridges have been examined by bathymetric mapping, grab sampling, coring, seismic profiling, SCUBA diving, and current monitoring. They are hemi-cylindrical sand bodies of recent age, resting on a pre-recent substrate. In troughs a thin, medium- to coarse-grained, pebbly lag veneers the substrate. Crests consist of a better sorted, medium- to fine-grained sand, while the flank sands are well sorted and fine- to very fine-grained.

The fair-weather hydraulic regime has been assessed by means of a direct-readout, orthogonal, current meter system. Five, 12- or 24-hour bottom stations were monitored. Wave surge and long period, coast-wise, residual currents were generally sub-equal in intensity, ranging from 0 to 20 cm/sec. Four stations yielded records of weak currents that could not be readily related to ridge building. SCUBA dives indicate that main fair-weather bottom adtivity is the slow migration of wave-generated ripples up to 5 cm high, obliquely shoreward across ridge crests. However, a station in the most landward trough recorded a current that appeared to be actively scouring the trough floor. During the station the wind built up from a calm to 25 knots from the northeast. Seas rose to 2 m, and began to break over the ridge seaward of the trough. A south trending bottom current of 20 cm/sec developed and continued despite the turn of the tide. Circumstantial evidence suggests that such strong south-trending currents dominate the inner shelf during storms, and are the ridge-building currents. Shortly after a storm, sand waves with a wavelength of 25 - 30 m and amplitudes of 1 - 2 m were observed on a

ridge crest. Cores reveal cross-bedded horizons up to 1 m thick within ridge crests. Second-order ridges on the flanks of some major ridges are asymmetrical towards the main crest, suggesting that during storms, south-trending bottom currents may diverge from trough axes and converge toward ridge crests.

ACKNOWLEDGEMENTS

The writer expresses his sincere gratitude to Dr. Donald Swift for his most helpful supervision of this research as head of the thesis committee. Appreciation is also expressed to Dr. John C. Ludwick for his valuable discussions and guidance. Further appreciation is expressed to Dr. Robert Byrne, Dr. Robert Cheng and Ronald Johnson as members of the thesis committee. John McHone helped greatly in obtaining field data. Special appreciation is expressed to my wife and family for their unselfish cooperative attitude and their understanding and help. Further appreciation is expressed to the captains of the R/V ALBATROSS, Capt. Robert Bray and Capt. Eugene Doty, and the captain and crew of the RANGE RECOVERER.

This study was supported by the National Science Foundation Grant GA-13837 and the Office of Marine Geology, U. S. Geological Survey. This thesis was typed by Mary Virginia Daniel.

TABLE OF CONTENTS

LIST OF FIGURES

LIST OF TABLES

INTRODUCTION

Purpose of Study

This study is designed to investigate the hydraulic regime of the inner shelf off False Cape, Virginia, and to determine its relationship to the underlying ridge and swale topography.

The topography of the False Cape area consists of a group of oblique-trending ridges which tie to the shore face in depths as shoal as 4 meters. Sanders (1962), Fisher (1967) and Payne (1970) have suggested that these ridges are relict Pleistocene beach ridges. However, Moody (1964) has mapped a similar ridge system off Bethany Beach, Delaware, before and after the Ash Wednesday storm of 1962, and determined the ridges had moved up to 70 meters in the interim. He concluded the ridges were large-scale, hydraulic bedforms, whose continued evolution during a period of sea level rise and shoreline recession gave rise to the offshore ridges. Shideler and others (in press) have obtained a radiocarbon date of 4,200 ± 140 years B.P. from a depth of 1.7 m on the flank of one of the False Cape ridges, suggesting a Holocene age for the ridge system.

It has been proposed that the False Cape ridge system is comprised of a Holocene sand sheet molded into large-scale hydraulic bedforms, probably formed in response to coast-parallel storm currents (Swift and others, in press). These authors have also suggested that the innermost ridge and trough of this system may be in a state of active formation, nourished by the eroding shore face. This study attempts to test these hypotheses by analysis of a grab sample net and by analysis

Figure 1. Bathymetry of the southern Virginia inner shelf, modified from Payne, 1970. Isolated highs with bases at 60 feet or above are stipled. Drawn by Richard Boehmer.

36°50'
36°40'
36°30'
75°50'
75°40'
75°30'
10-FM.

Figure 2. Bathymetry of the False Cape Study Area.

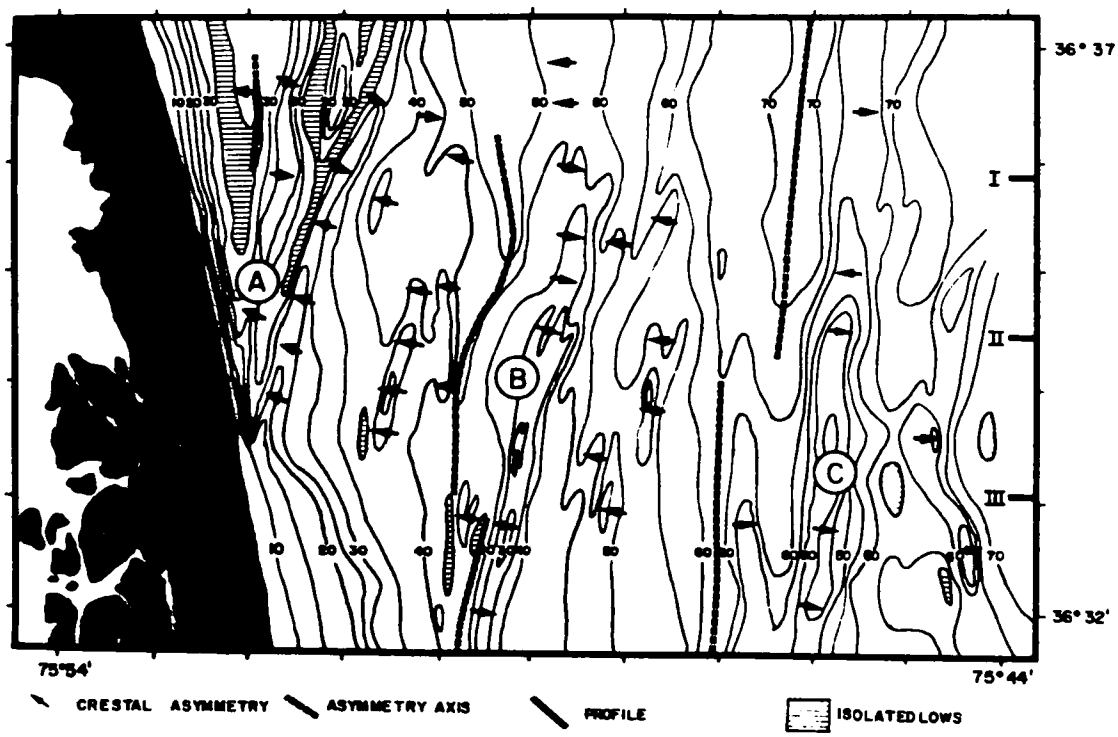
36° 37'
36° 32'
75°54'
75°44'
I
II
III
A
B
C
CRESTAL ASYMMETRY
ASYMMETRY AXIS
PROFILE
ISOLATED LOWS

Figure 3. Three dimensional drawing of ridge and swale topography at False Cape. Drawn by Swift.

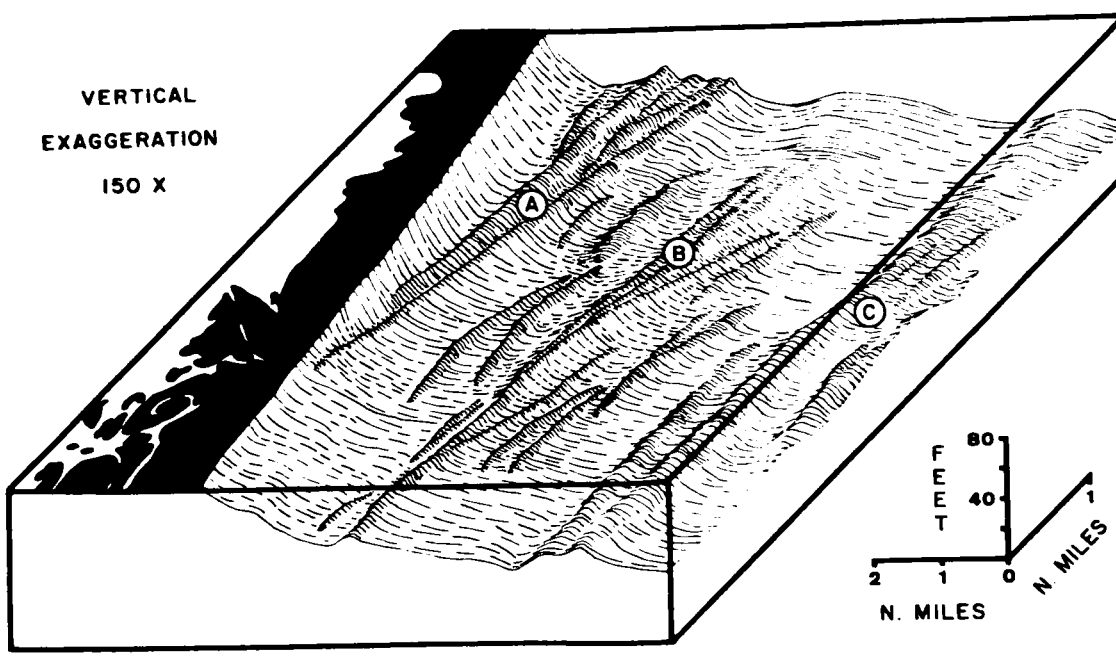
VERTICAL
EXAGGERATION
150 X
A
B
C
80
40
FEET
2
1
0
1
N. MILES
N. MILES

of the data from a series of bottom current monitoring stations.

Description of Study Area

False Cape, Virginia is a slight protusion on Currituck Spit just north of the Virginia--North Carolina boundary (Fig. 1). This barrier system has been considered by Pierce and Colquhoun (1970) to be a prograded spit from a former headland in the region of Oregon Inlet. Hoyt (1967) has argued that such barriers form as mainland beaches and are detached by rising sea level. Evidence of a former Albemarle River mouth in the area of Kitty Hawk, North Carolina (Swift and others, 1971, and Fisher, 1967) is compatible with the detachment origin.

The regional bathymetric map (Fig. 1) reveals a system of nearshore ridges with northward opening troughs in the vicinity of False Cape, Virginia. Just north and east of False Cape is another system of northeast-southwest trending ridges forming a complex configuration of ridges and troughs. A bathymetric map and three-dimensional diagram of the False Cape Ridge System (Figs. 2, 3) have been constructed from bathymetric data collected with an Edo depth sounder and a Cubic Autotape Precision Navigation system. The diagrams reveal three distinct systems of ridges and two distinct sectors of the shoreface region. The upper, steeper sector intersects with the lower, gentler sector at approximately 20 feet (6 m). Two of the ridges (A ridge and B ridge) emerge from this upper shore face sector and traverse the lower sector, while the outermost ridge system (C ridge) paralleling the other two, rests directly on the inner shelf floor (Swift and others, 1971).

Second order ridges on the flanks of major ridges appear to have a subdued asymmetry with steeper slopes facing away from major troughs

Figure 4. Comparison of False Cape topography from 1922 U.S.C. & G.S. survey (dashed lines) and a 1969 survey (solid lines).

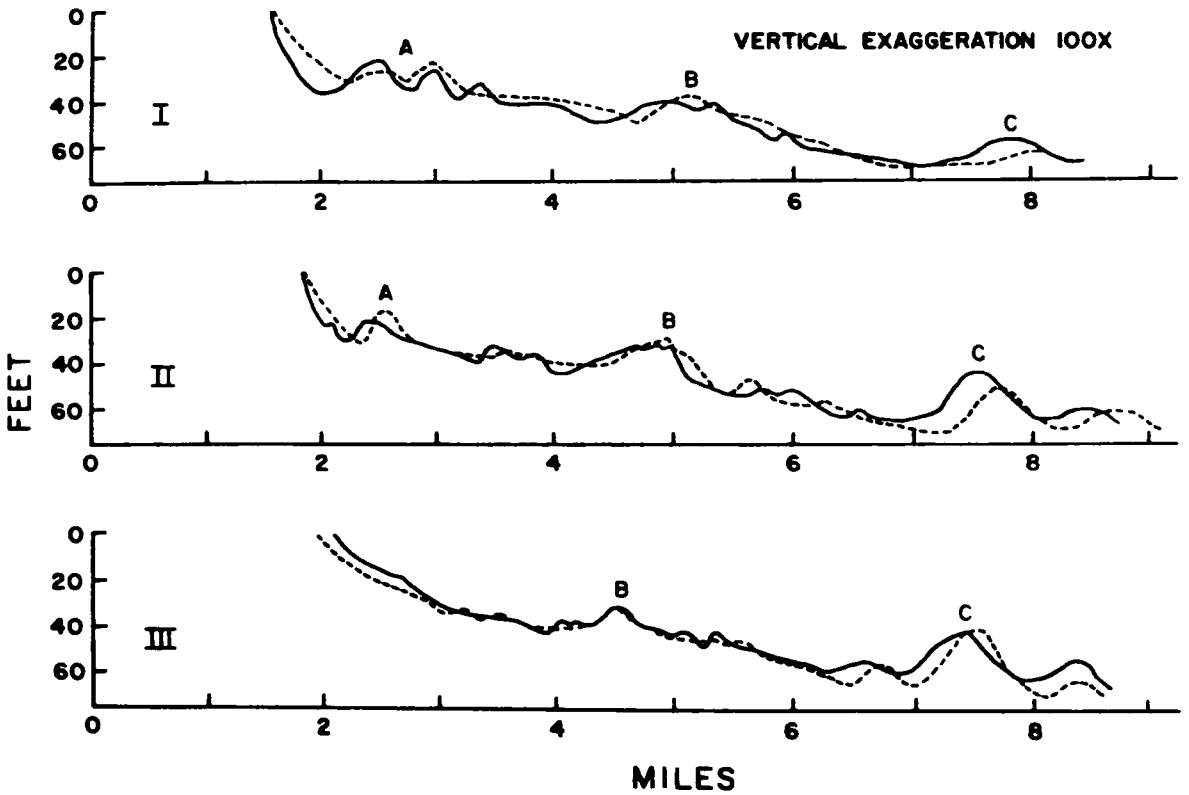
VERTICAL EXAGGERATION 100X
FEET
0
20
40
60
I
II
III
A
B
C
0
2
4
6
8
MILES

(Fig.2), and the ridges tend to decrease in relief toward the north (Swift and others, 1971). These authors have also noted that the troughs are generally flat-floored and much broader than the narrow rounded crests. "Hence profiles through the system resemble profiles through trochoidal surface waves, or perhaps more accurately, solitary waves."

Comparison of a bathymetric map drawn from a 1922 U.S.C.&G.S. boat sheet and the detailed bathymetric map made in 1969 (Fig. 2) implies that within this period, the ridge crests have at numerous points moved landward with maximum displacements in excess of 150 yards (Fig. 4). Swift and others (1971) offer a discussion of the caution which must be observed in such comparisons; however, this net movement is supported by Felton (unpublished manuscript, Norfolk District Corps of Engineers) on the South Virginia coast and Moody (1964) has observed motion of near-shore ridges in a similar region off Bethany Beach, Delaware.

Figure 5. Map showing grab sample net (open circles) and seismic profile transects (solid circles).

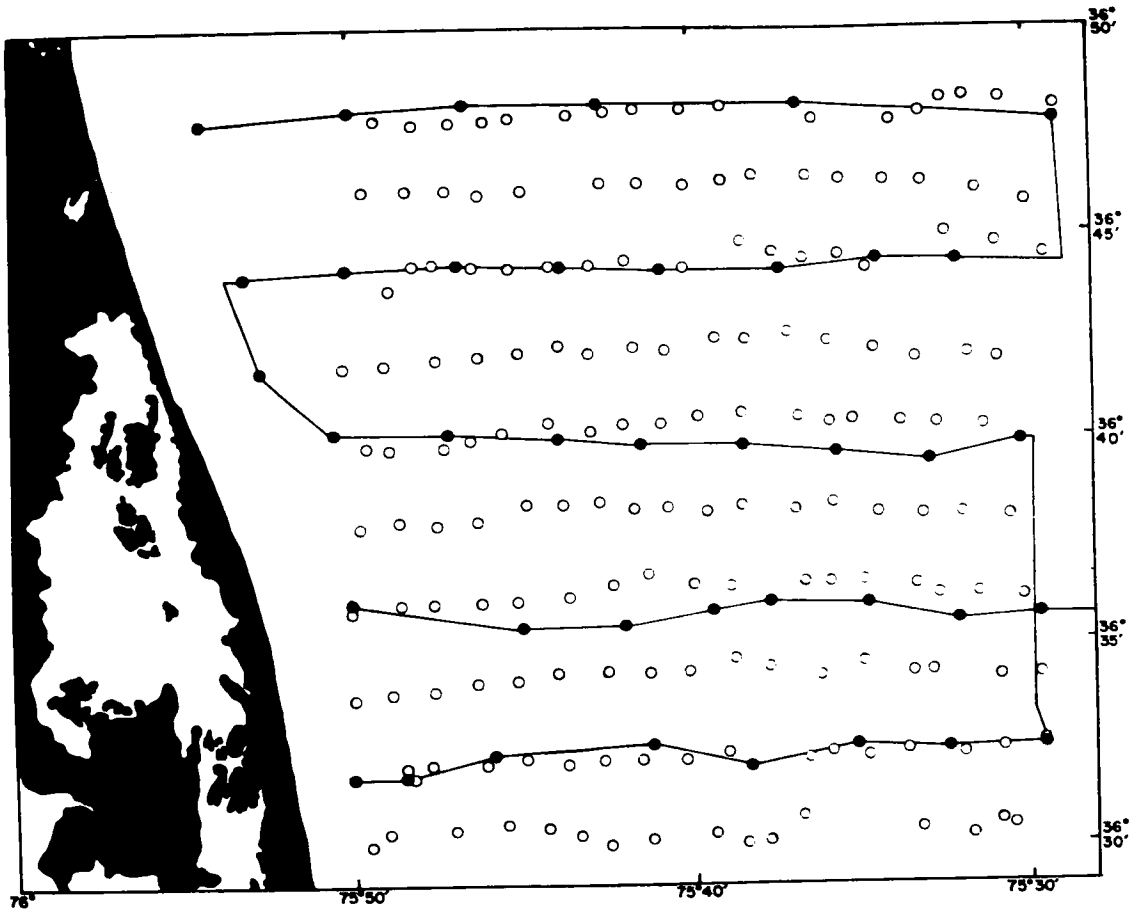
36°
50′
36°
45′
36°
40′
36°
35′
36°
30′
75°50′
75°40′
75°30′

Figure 6. Median grain size distribution map of False Cape study area with prominent ridges surimposed.

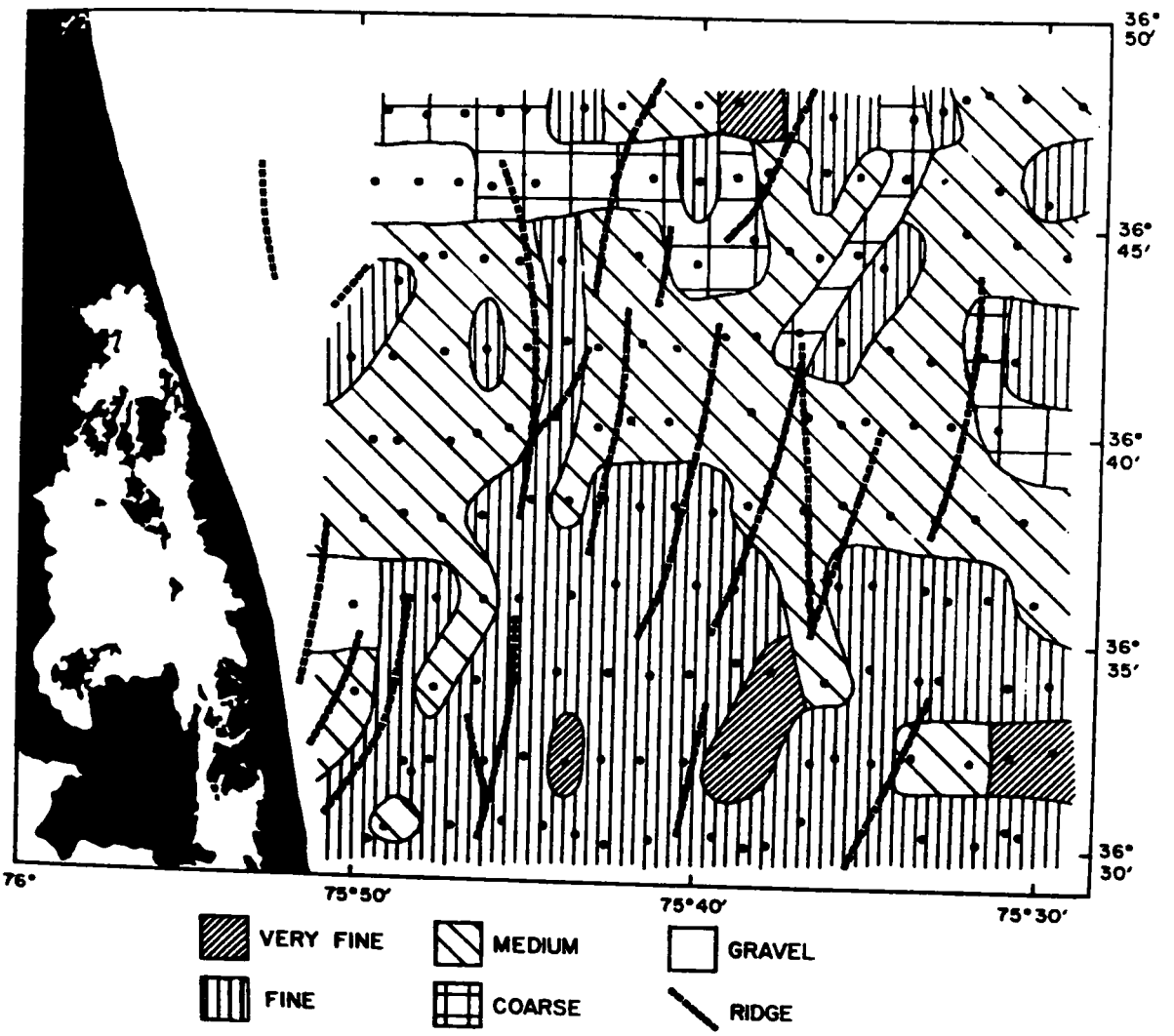
36° 50′
36° 45′
36° 40′
36° 35′
36° 30′
76°
75°50′
75°40′
75°30′
VERY FINE
FINE
MEDIUM
COARSE
GRAVEL
RIDGE

GEOLOGIC FRAMEWORK OF THE STUDY AREA

Grain Size Reconnaissance

A 36 km by 34 km area (Fig. 5) on the inner Virginia shelf off Virginia Beach was sampled with a Shipek grab sampler during the 1969 cruise of the RANGE RECOVERER. One hundred and seventy samples were obtained on 10 east-west transects. The transects were 4 km apart in a north-south direction and the samples on the east-west transects were 2 km apart. Each sample was placed in a quart container labeled with the depth and position of each sample point. Depth was determined from the ship's depth recorder and navigation and positions were initially controlled by Loran A; however, due to obvious discrepancies in the early evening, radar range and hearing fixes were utilized.

The samples were prepared for use in a modified Woods Hole Rapid Sediment Analyzer (RSA) as described by Sanford and Swift (in press). The preparation included splitting the sample to a workable volume, removing the clay and fine fraction with a Calgon solution, removing the shell, sieving out anything greater than -1ϕ and micro-splitting to approximately a 3 gram sample.

From the grain size frequency distribution plots of the samples, the median diameter was determined for each sample dropped in the RSA. These ϕ values were compared with the Wentworth size classes and categorized mud, very fine sand, fine sand, medium sand, coarse sand and gravel (Fig. 6).

The median diameter distribution does suggest a subtle small-scale pattern of North-South trending belts. This pattern is surimposed on a

Figure 7. Index map of study area. The map illustrates the location of seismic profile network and vibracore transect. From Shideler and others, in press.

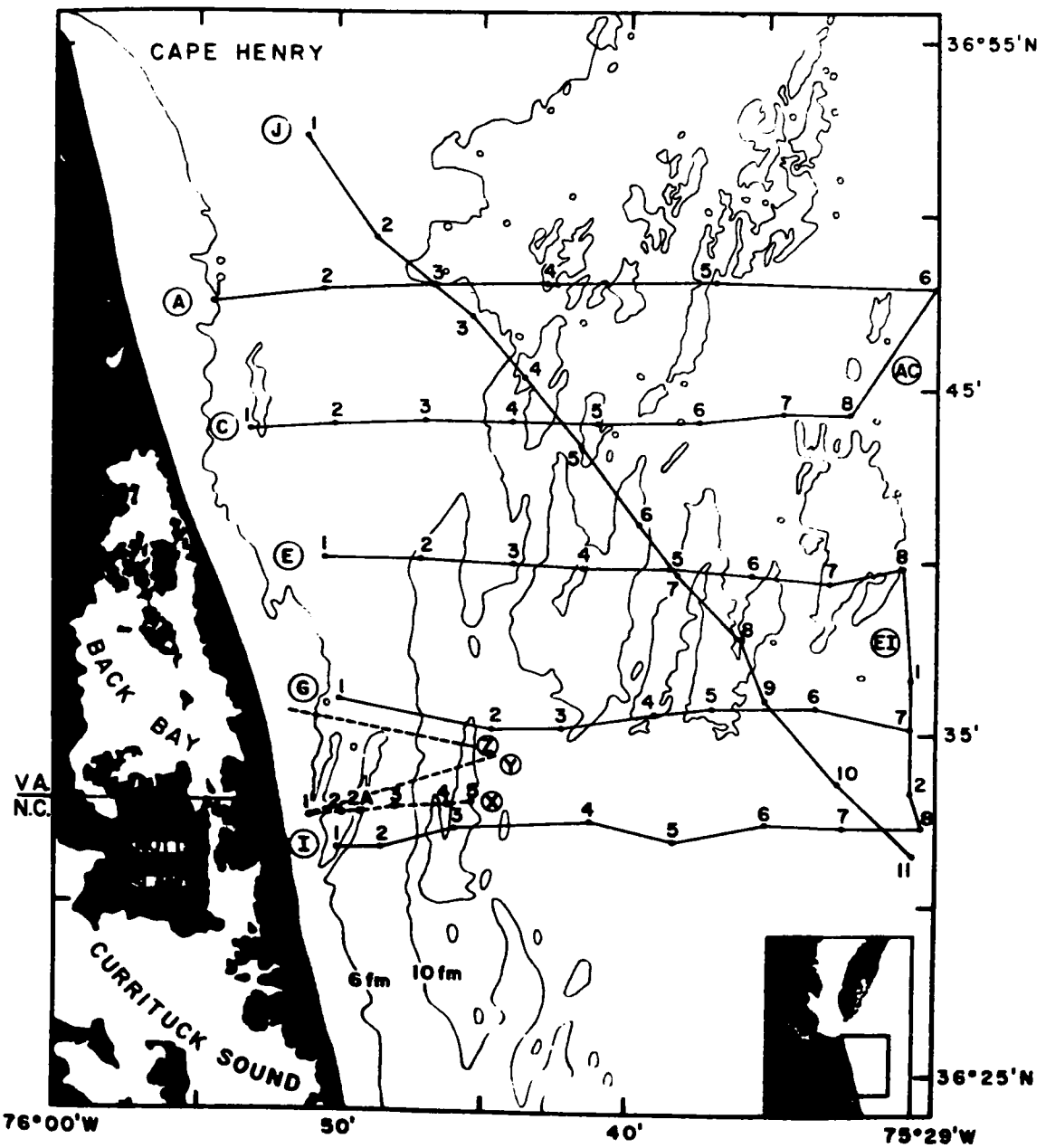
CAPE HENRY
36°55'N
45'
35'
36°25'N
76°00'W
50'
40'
75°29'W
VA.
N.C.
BACK BAY
CURRITUCK SOUND
6 fm
10 fm
J
A
C
E
G
I
AC
EI
X
Y
Z

Figure 8. Stratigraphy of False Cape area, as revealed by seismic reflection probe and vibracores (lower line).

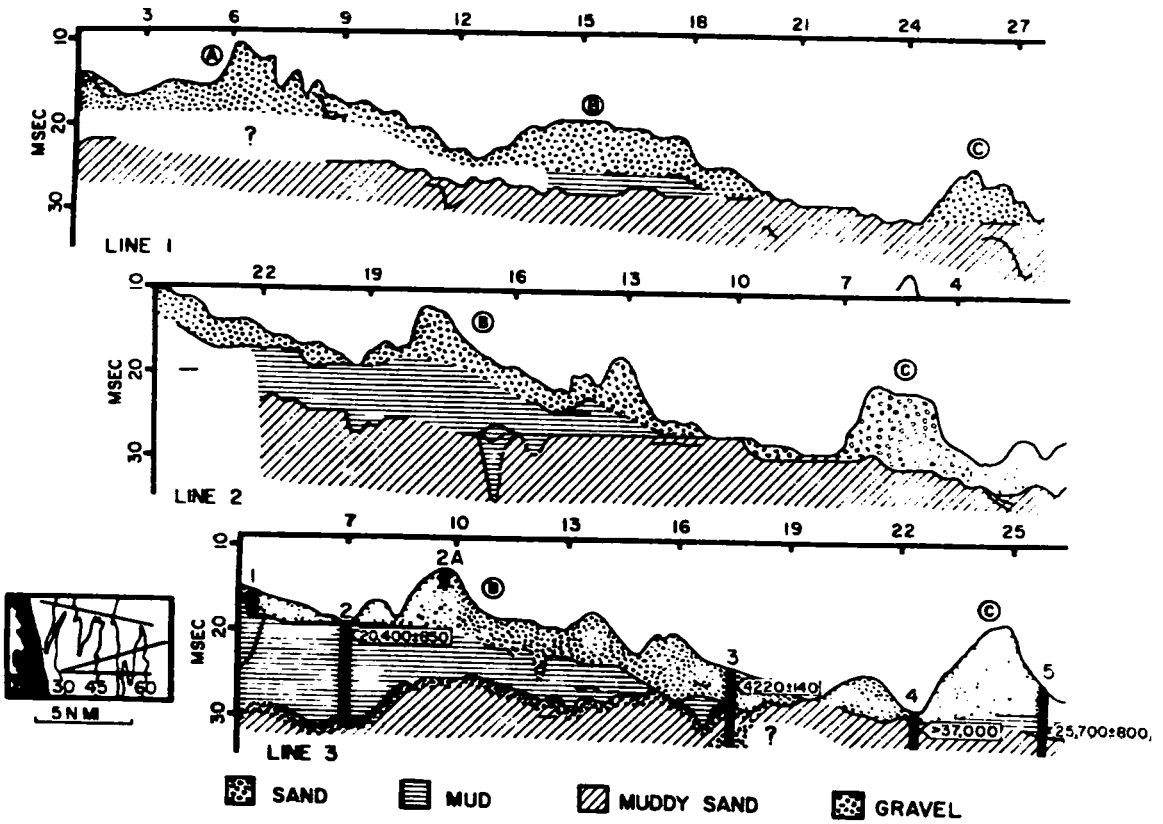
3 6 9 12 15 18 21 24 27
MSEC
LINE 1
22 19 16 13 10 7 4
LINE 2
7 10 13 16 19 22 25
2A
20,400±850
220±140
>37,000
25,700±800,
LINE 3
30 45 60
5 NMI
SAND
MUD
MUDDY SAND
GRAVEL

large-scale pattern of definite coarsening to the North. There is no obvious correlation of grain size with topography. However, this appears to be a consequence of the wide spacing of the sample net, since information obtained from scuba diving and other grab sampling indicates close correlation of topography and grain size (Swift and others, in press). Trough axes tend to be floored with a coarse, pebbly sand lag overlying a firm pre-recent substrate. Ridge crests are composed of well-sorted medium to fine sand, ridge flanks consist of fine to very fine sands.

Stratigraphy

The False Cape area has been sampled by a continuous seismic reflection survey over the entire study area, by five vibracores along the South transect and by several shallow hand-driven cores on monitoring stations along the south transect. The seismic survey profiles have been discussed at length by Shideler and others (in press). Their work indicates that the Post-Miocene section off the False Cape area has an average thickness of 27 meters and consists of three distinct sedimentary sequences separated by unconformities.

The vibracores, which were used as a supplement to the seismic profiles, were obtained along the False Cape South transect (Fig. 7) during the summer of 1970 aboard the R/V EASTWARD. Detailed subsurface data were obtained from analysis of these cores (Fig. 8). The cores ranged in length from 3 to 10 m and were 9 cm in diameter. They were cut longitudinally in half and sampled within a short period to assure natural color and texture. Impregnations were made of pertinent sections of the cores and samples were taken for analysis of grain size and faunal assemblages. The impregnation medium was an epoxy mixture described by Burger,

Figure 9. Hand-hammered core from crest of B ridge, Sample 2A, Fig. 7.

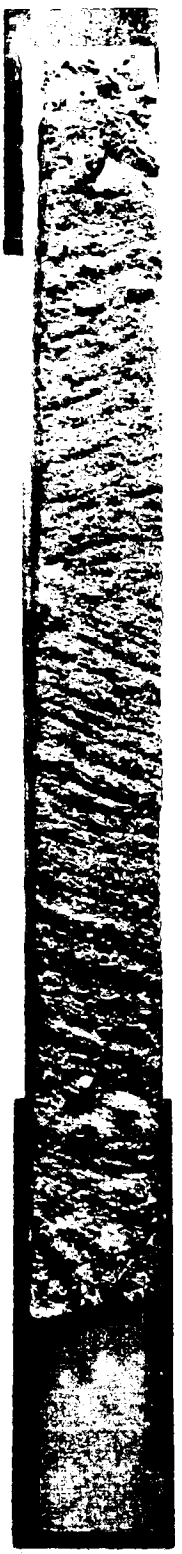

Klein and Sanders (1969).

Shideler and others (in press) have interpreted the oldest post-Miocene sequence as a pre-Wisconsinan and early Wisconsinan deposit with a radiocarbon age of greater than 37,000 years B.P. Seismic profiles and cores suggest the deposit contains both a transgressive fluvial complex and a regressive coastal barrier complex consisting of largely muddy, fine-grained sand with frequent lenticular stratification and local channeling.

Two radiocarbon dates were obtained for the intermediate sequence ranging from 25,700±800 years B.P. at its base (25 m below sea level), to 20,400±850 years B.P. at its top (15 m below sea level as an outlier), indicating a Pleistocene age. The sequence is characterized by relatively uniform horizontal stratification comprised mainly of mud and appears to represent a regressive paralic-neritic sequence developed at the end of the mid-Wisconsisan interstadial (Shideler and others, in press).

The youngest sequence has yielded a single radiocarbon date of 4020±200 years B.P. from an articulated Mercenaria sp. cored at a depth of 1.5 m on the seaward flank of B ridge. It comprises the modern sea floor sand. This discontinuous sand blanket appears to have formed during the Holocene as a sea floor lag, generated by shore face erosion of a retrograding barrier coast complex. It has been molded into the ridge and swale topography by the Holocene hydraulic regime (Swift and others, in press).

A detailed discussion of the lithology, radiocarbon dates and paleontology is found in Shideler and others (in press). To supplement the vibracore sampling, hand-hammered cores were obtained on the berm and on the crest of B ridge (Fig. 9). Sample 2-A (Fig. 9) shows definite

cross bedded horizons up to 1 m thick within B ridge crest suggesting recent active sand waves.

Figure 10. Position of the current meters, the wave gage and the compass on the triangular frame.

Figure 11. Close-up of Bendix Q-18 current meter showing contour of blades.

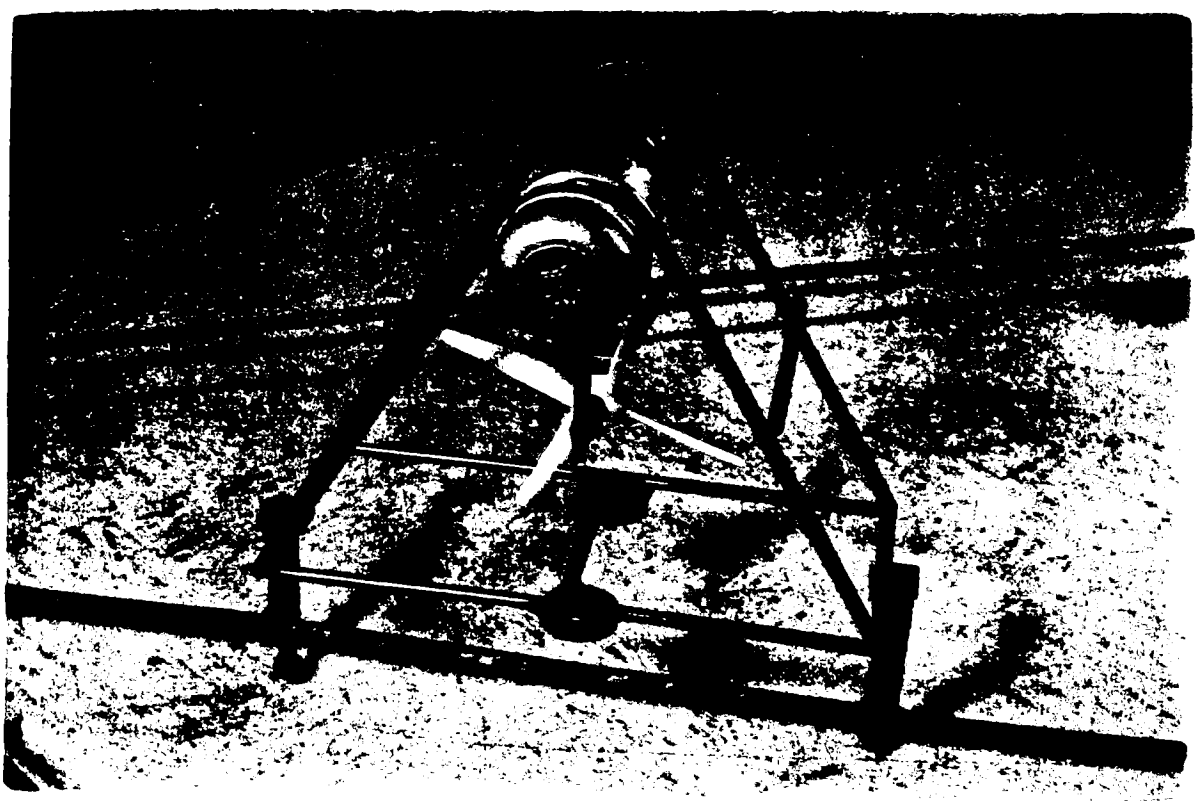

Figure 12. Bendix, Marine Advisers current speed and direction readout boxes.


CURRENT
DIRECTION

FIELD METHODS

The monitoring program, which constituted the major portion of the research undertaken, was conducted with the use of a Bendix Marine Advisers Q-18 current meter system and a Hydroproducts Wave and Tide Analyzer system mounted on a special triangular frame (Fig.10). The Bendix Q-18 current meter system is an orthogonal, cosine response current meter. It utilizes an impeller assembly of small mass that responds quite rapidly to changes in current velocity and, due to the contour of the blades, it responds just as rapidly to changes in direction of flow (Fig.11). The meters are coupled with an electromagnetic compass placed on the triangular frame (Fig.10). This sensor gives constant readout of the orientation of the meters. The current meters are mounted at right angles to each other approximately .6 m apart with their axes in the horizontal plane. With this horizontal configuration, the velocity very near the bottom can be calculated.

The readout package used with the Q-18 meters offers two identical channels of electronic processing, one for each of the two signals supplied by the meters. The signals are displayed on two meters and a dual-channel, Rustrak strip-chart recorder (Fig.12). The meters are calibrated in knots and a choice of integration time constants are available. There are three positions: 1 (short time constant), 2 (medium time constant), and 3 (long time constant). In position 1, a short integration time offers observations of specific pulses from the impellers of the current meters. Position 2 suppresses the response to specific pulses

Figure 13. Hydro Products Wave and Tide Analyzer readout box.

to a smoother meter readout that is representative of the normal motion and magnitude of the near-bottom current. Position 3 must have flow in a single direction for an extended period of time, individual pulses being almost entirely obliterated. The data obtained with the Q-18 system at False Cape, Virginia was obtained in time constant position 2.

The Hydroproducts wave and tide analyzer system consists of a small pressure transducer mounted on the triangular frame and a special meter readout package for shipboard use (Fig.13). The transducer consists of a special strain gage assembly which sends a signal to the shipboard meter system. The pressure variations are displayed on the meter which displays instantaneous wave height, characteristic wave height, average wave period and tide level. Performance of the system has been unsatisfactory up to this time, having experienced corrosion shorts in the circuitry, water in the power cable and other minor mishaps. Therefore no data was obtained in coordination with the current meter monitoring. All wave information has been obtained from personal observations.

The triangular frame is approximately 7 feet on a side and utilizes Volkswagen hub-caps as skids (Fig.10). From Figure 10 the position of the meters, compass and wave gage can be determined. The height above the bottom to the axis of the current meters is approximately 10 cm; this value will fluctuate depending on the size of ripples and the character of the bottom. Diver observations and previous calibration tests indicate that the frame does not significantly affect the slowly oscillating bottom currents measured by the meters.

The current meters were taken to Johns Hopkins University to the Chesapeake Bay Institute flow tank for preliminary calibration and tests.

FIGURE 14. Calibration plot of Bendix Q-18 meters with the CBI flow tank.

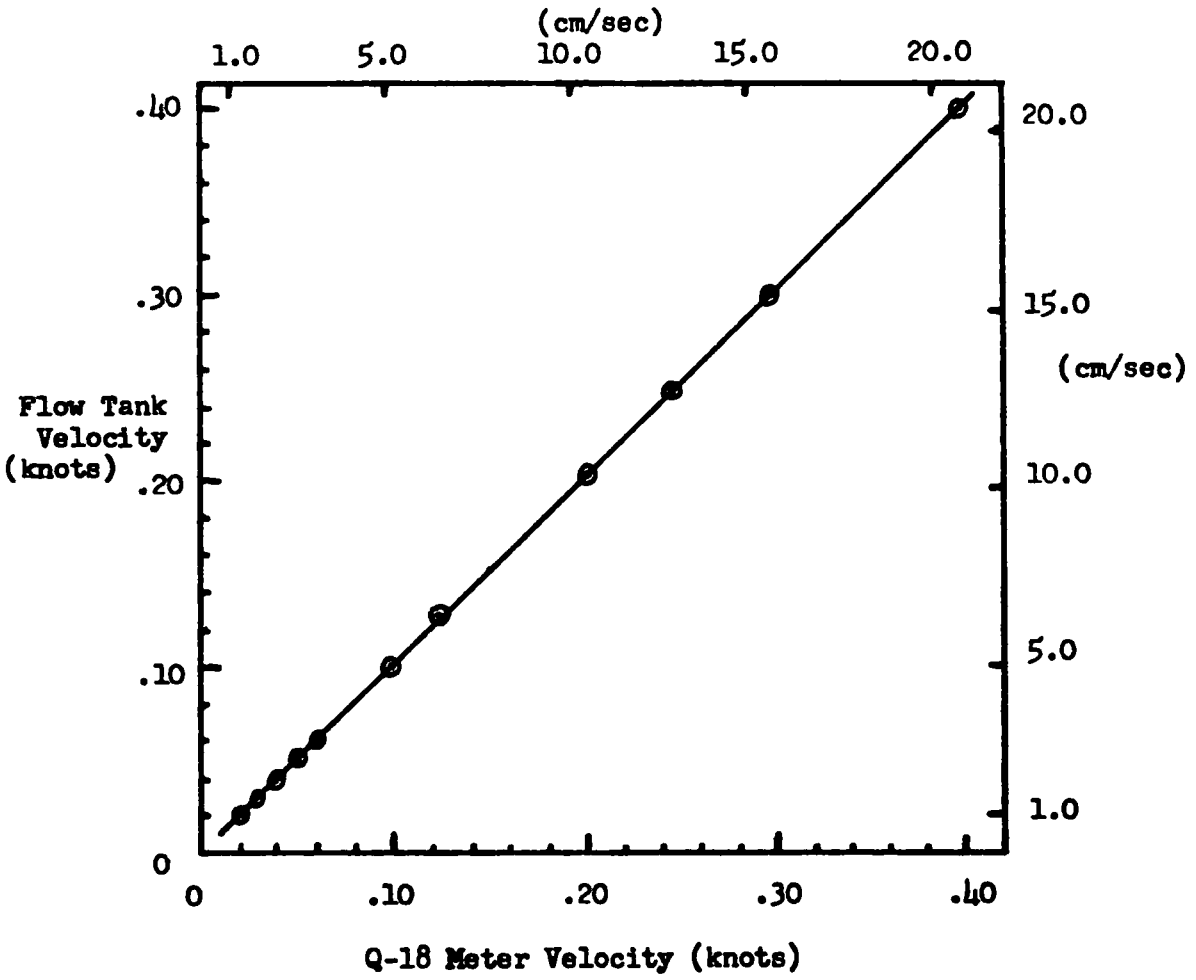

Figure 15. Mounting and position of Bendix Q-18 current meters in the CBI flow tank.

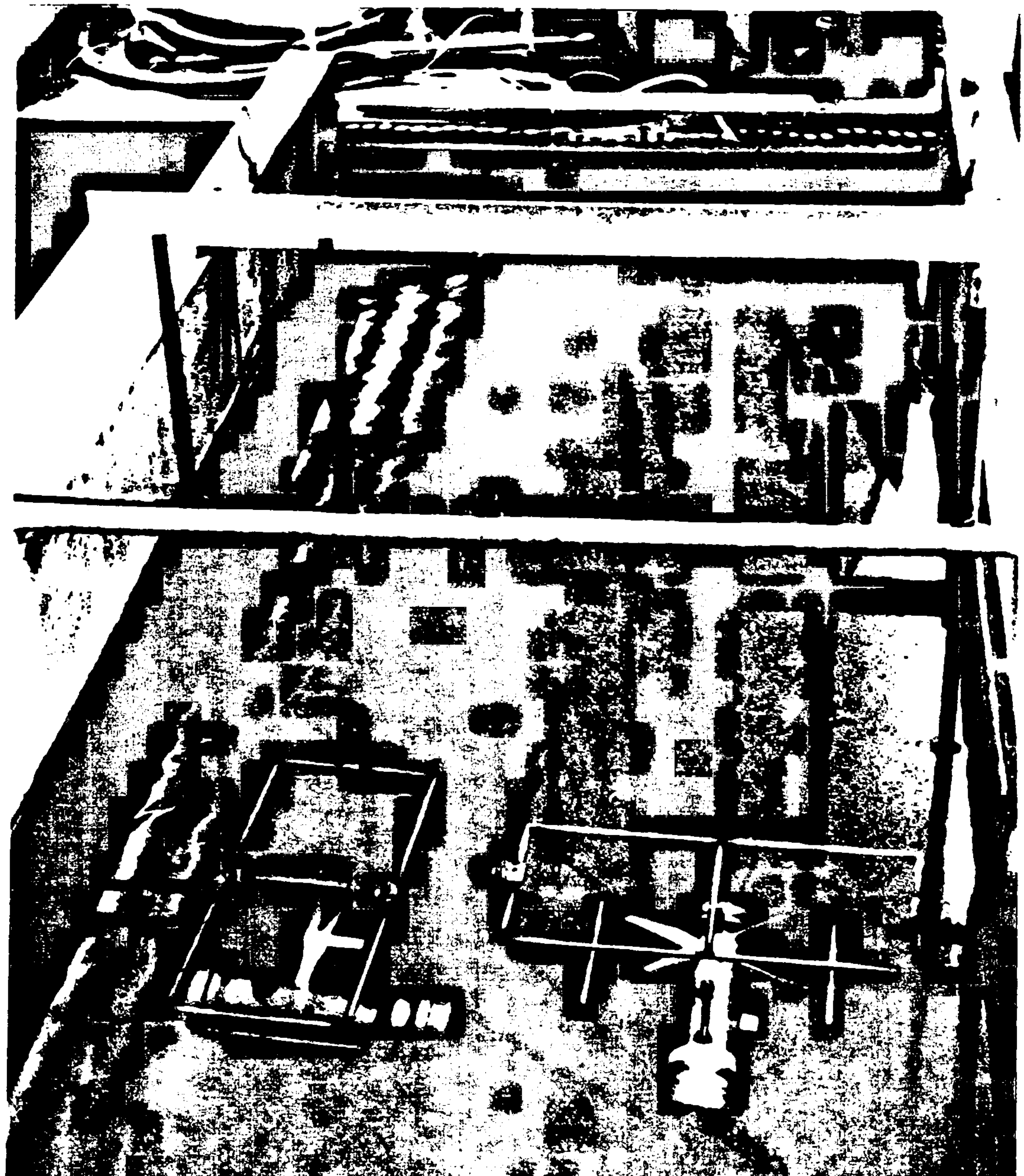

ANGLE OF HOLDING ROD AND FLOW	RED METER VALUE	WHITE METER VALUE	VELOCITY FROM METERS	VELOCITY OF TANK
0	.00	.20	.20	.20
25	.08	.18	.199	.20
30	.10	.17	.197	.20
45	.14	.14	.198	.20
60	.17	.10	.197	.20
75	.19	.05	.197	.20
90	.20	.00	.20	.20

TABLE 1 Calibration of Bendix Q-18 meter response to cosine of angle of flow in the CBI flow tank. "Red" meter axis initially is facing the tank wall; "white" meter axis is facing the current (see figure 10).

Figure 16. Comparison of bathymetry of False Cape with rose diagrams of monitoring stations. Current meter stations numbered from left to right.

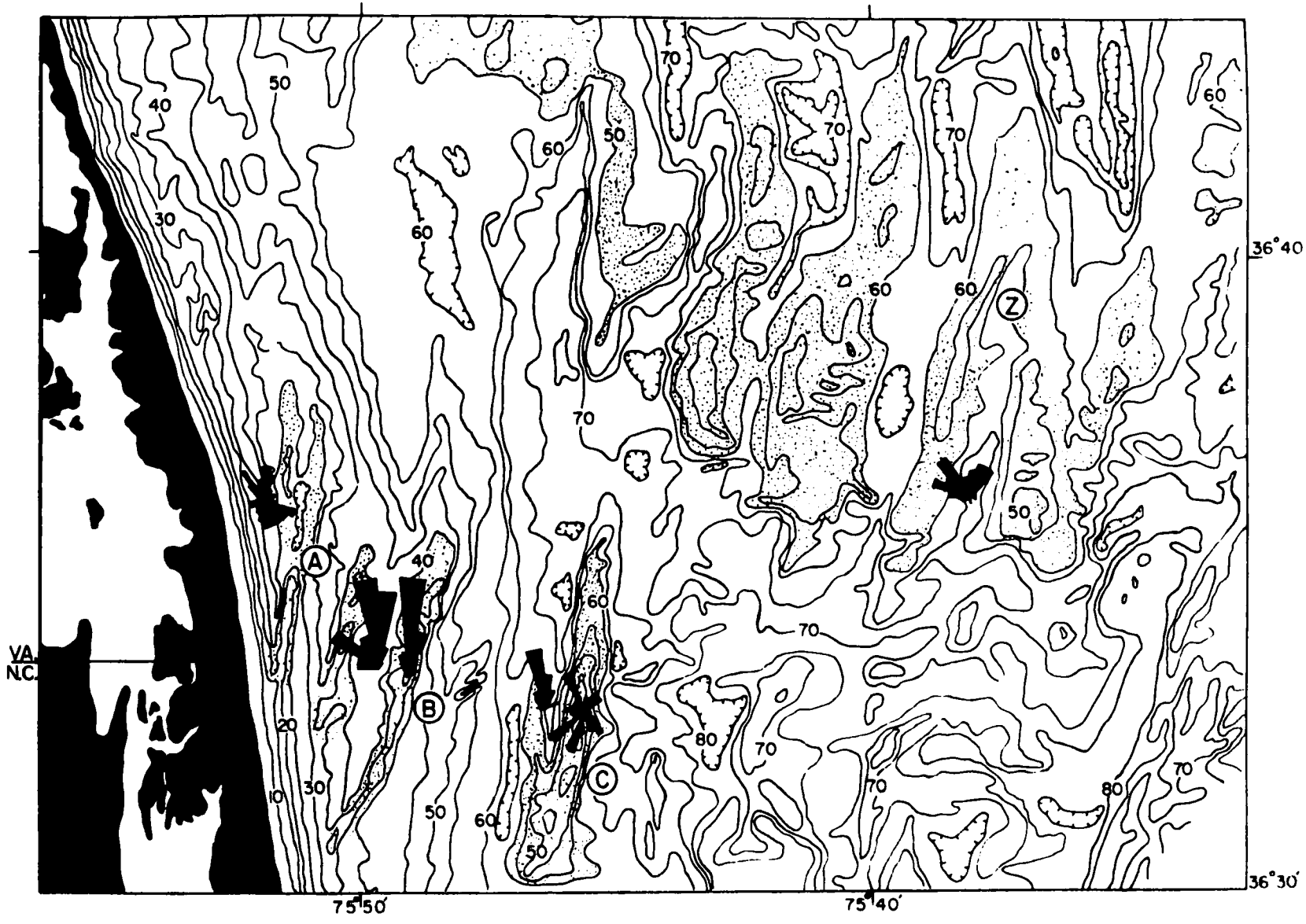
VA.
N.C.
A
B
C
Z
10
20
30
40
50
60
70
80
36°40'
36°30'
75°50'
75°40'

The meters have a threshold of response of 1.03 cm/sec or .02 knots and all velocities calculated from the two meters very closely correlate with the known velocities of the flow tank (Fig.14). The meters were positioned in the tank at approximately mid-depth (Fig.15), at right angles to each other as they are placed on the triangular frame. The system was rotated slowly through 90° with the Rustrak recorder operating, and the results correctly showed a cosine response from the meters with respect to the flow angle of the tank (Table 1). The meters were then rotated 90° more to test response in the opposite direction. This test was equally satisfactory.

Eight 24 hour monitoring stations were attempted in the False Cape study area at various locations (Fig.16). Of these 8 stations, six were usable. The other two were lacking either positioning information about the meters or orientation data for the compass. Four of the six workable stations were undertaken on an east-west transect in the False Cape Ridge system just south of the Virginia-North Carolina line ("False Cape South Transect" on Fig. 7). An additional station was recorded on the Virginia Beach Ridge system due east of False Cape at "Z" ridge (Fig. 16). A final station was monitored due east of a large range pole emplaced by the Hastings-Raydist Company, in A trough of the False Cape Ridge System.

Two different vessels were used to obtain the data from the stations. Three of the stations were monitored from the R/V ALBATROSS, a 20 m Army T-boat operated by the Institute of Oceanography, Old Dominion University. The other three stations were made aboard the USNS RANGE RECOVERER, a 55 m vessel operated by NASA-Wallops as a telemetering and recovery ship. A complete description of each monitoring station

Figure 17. Representative 30-minute current meter station readout from Rustrak strip chart recorder showing sampling interval, time of day, and the date.

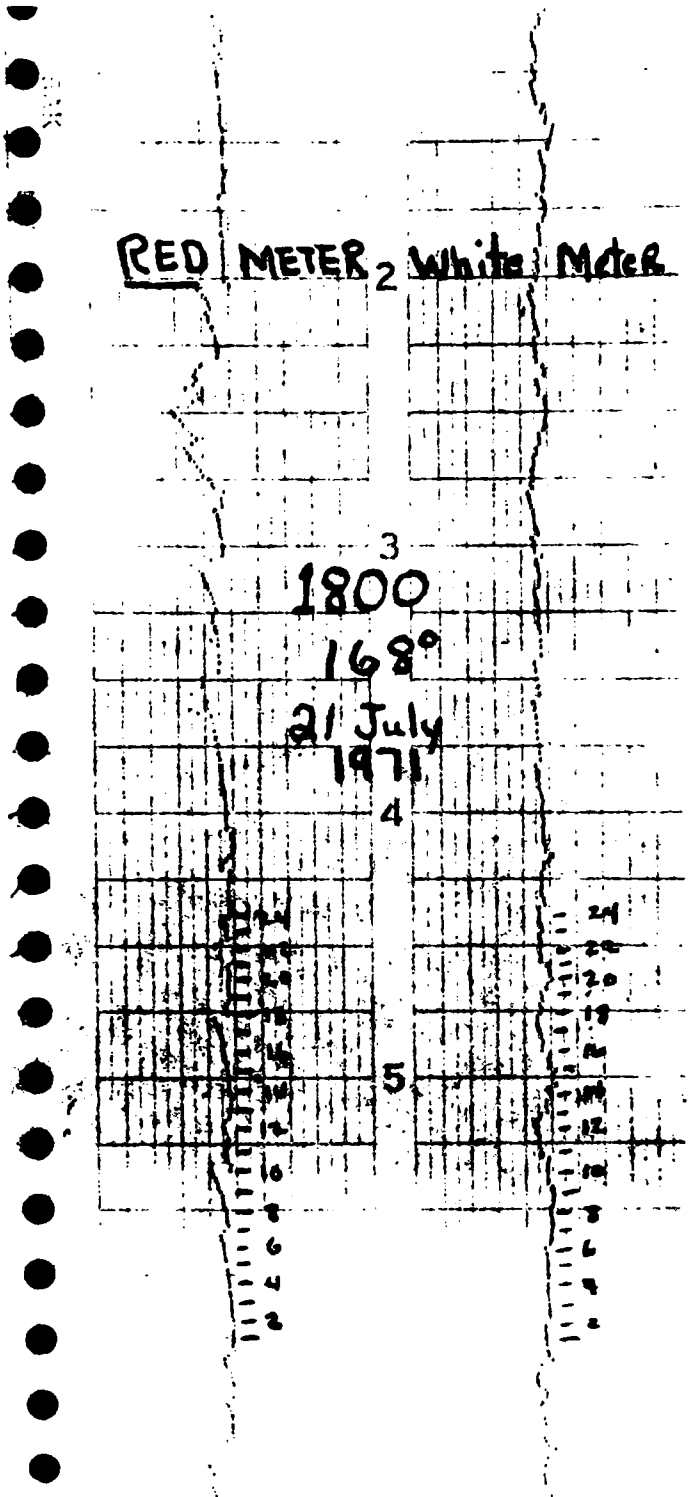
RED METER 2 White Meter
3
1800
168°
21 July
1971
4
5

including time, date, weather, wave conditions and bottom character is found in Appendix I.

Data Reduction

The data from the six monitoring stations were printed on recorder chart paper by the Rustrak dual-channel recorder. The printout was a contact on the paper every half second for each meter. The paper offers a 2.5 cm full scale deflection for each channel (Fig. 17). Consequently, the task of analyzing such a small record offered many difficulties. Figure 17 is a representation of a standard sampling station, at which velocities were sampled for 3 continuous minutes every 30 minutes. The figure shows the proper time, the meter orientation in degrees, and the date. Each vertical line running the length of the chart paper equals .10 knots (5.5 cm/sec). The tick marks and numbers are the normal procedure used to analyze the output. The left side corresponds to the "Red" meter (a color code coordinating each of the meters with a particular meter in the readout box) and the right channel corresponds to the "White" meter. A magnifying glass was used to assure clarity in estimating to the nearest .01 knots (.55 cm/sec) and was mandatory to count every fifth point of the output . Twenty-four readings per station gives a full minute of data and using every fifth point reduces aliasing of the oscillatory character of the current flow output. More data points per 30 minute station does not significantly alter the mean velocity and direction values.

When 24 values each were obtained for both the "Red" and the "White" meters, the pairs of values were entered into a Monroe 1665 computer programmed to calculate the vector of speed and direction. These values

Figure 18. Sample data sheet for each 30 minute station.

CURRENT METER DATA SHEET

TIME 1830 – DATE 15 July, 1970 COMPASS 175°

	u	D		u	D
R -.09 W +.09	.13	155	R -.10 W +.10	.14	155
R -.05 W +.03	.06	141	R -.13 W +.01	.13	114
R -.02 W -.08	.08	34	R -.10 W -.04	.10	88
R -.03 W -.05	.06	51	R +.01 W +.01	.01	245
R -.06 W 0	.06	110	R +.02 W +.05	.05	221
R -.12 W +.02	.12	119	R 0 W +.04	.04	200
R -.10 W +.02	.10	121	R -.12 W +.03	.12	124
R -.09 W +.02	.09	122	R -.10 W +.01	.10	116
R -.08 W -.01	.08	103	R +.01 W -.08	.08	13
R -.07 W -.01	.07	102	R +.02 W +.01	.02	263
R -.02 W -.07	.07	36	R 0 W +.06	.06	200
R -.02 W +.01	.02	137	R -.09 W +.08	.12	152
R -.03 W +.08	.08	179	R -.10 W +.03	.10	127

Figure 19. Example calculation of mean direction from 1 minute record of 30 minute station.

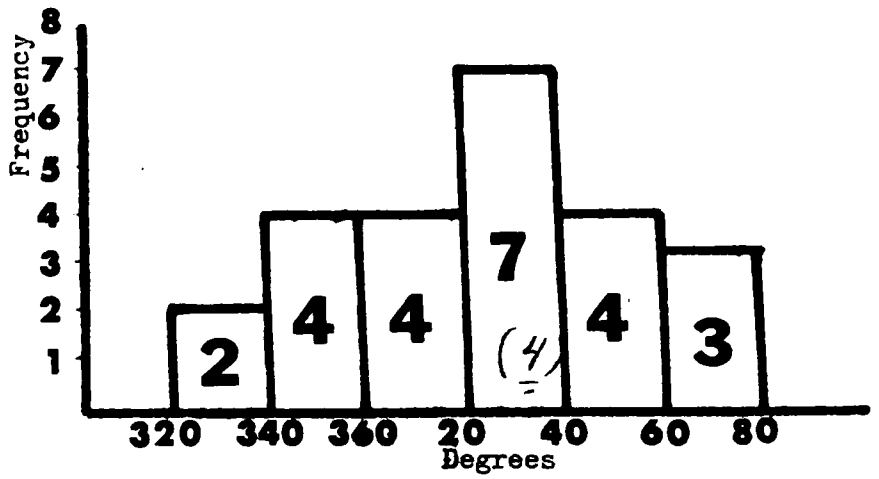

A	b	Ab
2	-3	-6
4	-2	-8
4	-1	-4
7	0	0
4	1	4
3	2	6
24=N		-8

$m_c^\circ = 20^\circ$

$M_m^\circ = 30^\circ$

$\frac{-8}{24}(20) + 30 = 23^\circ = \bar{D}$

Figure 20. Progressive vector diagram of Station 1 in A trough. See Appendix I. The bottom residual is 2.6 cm/sec toward the southeast (130°).

N
end

Figure 21. Progressive vector diagram of Station 2 in the landward trough of B ridge. See Appendix I. The bottom residual is 3.6 cm/sec toward the northwest (345°).

end
N

Figure 22. Progressive vector diagram of Station 3 on the crest of B ridge. See Appendix I. The bottom residual is 3.6 cm/sec toward the north (010°).

Figure 23. Progressive vector diagram of Station 4 in the landward trough of C ridge. See Appendix I. The bottom residual is 3.6 cm/sec toward the north (359°).

N
end

Figure 24. Progressive vector diagram of Station 5 on the crest of C ridge. See Appendix I. The bottom residual is 1.0 cm/sec toward the west (264°).

N
end

Figure 25. Progressive vector diagram of Station 6 in Z ridge trough. See Appendix I. The bottom residual is 3.6 cm/sec toward the northwest (347°).

end
N

were they split into velocity and direction columns (Fig. 18) to be statistically analyzed. Velocity values were added together and divided by the number of values to obtain a mean velocity ($\bar{U}$) per 30 minute station. However, according to Pincus (1956), orientation data such as direction of the current vector offers difficulty in making the proper choice of calculations to obtain the optimum results. The difficulties arise due to the discontinuous function of compass direction values (0° to 360°). A method described by Krumbein (1939) was selected, in which the directions are grouped into classes of usually 20° and a moment analysis is performed on the resultant histogram (Fig. 19). An equation was then used which related both the mid-point of the modal class and the distributions about this modal class and derives a mean value of the direction data. The equation is:

$$M^{\circ}_{m} + \left[\frac{\Sigma(Ab)}{N}\right] m^{\circ}_{c} = \bar{D}$$

where M°_{m} is the midpoint of the modal class, A is the number of values in each interval, b is the arbitrary positive or negative value assigned each interval, N is the summation of A, m°_{c} is the class interval (usually 20°) and $\bar{D}$ is the mean direction.

The calculations of mean velocity and mean direction were compiled for each monitoring station and plotted as a progressive vector diagram (Figures 20, 21, 22, 23, 24, 25). A progressive vector diagram is a graphic method of showing a time series of current velocity and is constructed by adding successive current vectors (Caster, 1969). From this diagram, a calculation of the total residual experienced over the monitoring period can be made by measuring the resultant vector connecting the tail of the first vector with the head of the last vector. The residual is then

determined by dividing the value of the resultant by the total number of vectors from the diagram (total number of 30 minute readings). To complement the progressive vector diagram and offer more information about trends of the current regime being measured, a rose diagram of the direction was constructed on the progressive vector diagram (Figures 20, 21, 22, 23, 24, 25).

HYDRAULIC REGIME OF THE CHESAPEAKE BIGHT: A LITERATURE SURVEY

The general currents of the Chesapeake Bight display a complex response to salinity and temperature gradients of the water column, and to the wind. To understand this response requires a knowledge of the seasonal changes that occur within the water column and seasonal changes of the speed and direction of the wind.

Seasonal Physical Properties of the Water Column

Summer Conditions

Harrison and others (1967) have attempted to determine the seasonal changes that can occur in the Chesapeake Bight water column. Their predictions are based on measurements of water column stability from the summer of 1963 through December of 1964 (Harrison and others, 1967, Fig. 7) and previous work undertaken by Bumpus (1957), Joseph (1960) and Norcross and others (1962). The summer water column conditions are characterized by high stability, and strong stratification, with a thin well-mixed warm surface layer overlying a strong vertical density gradient. When the summer stratification is developed, the transfer of energe (in the form of turbulence) through the thermocline is effectively inhibited (Harrison and others, 1967). Fluctuations in river run-off in the form of effluent from the Chesapeake Bay mouth vary the salinity of the shelf waters (Norcross and others, 1962). Harrison notes that maximum sustained river run-off occurs in spring, but this increased flow does not reach the shelf until summer due to lagging within the estuary system (Howe, 1962).

Figure 26. Representative wind roses of summer and winter winds. Numbers above each rose represent the number of six-hour periods of calm. Arrow represents vector resultant direction of wind movement. After Harrison and others, 1967 and Beach Erosion and Hurricane Study, 1967.

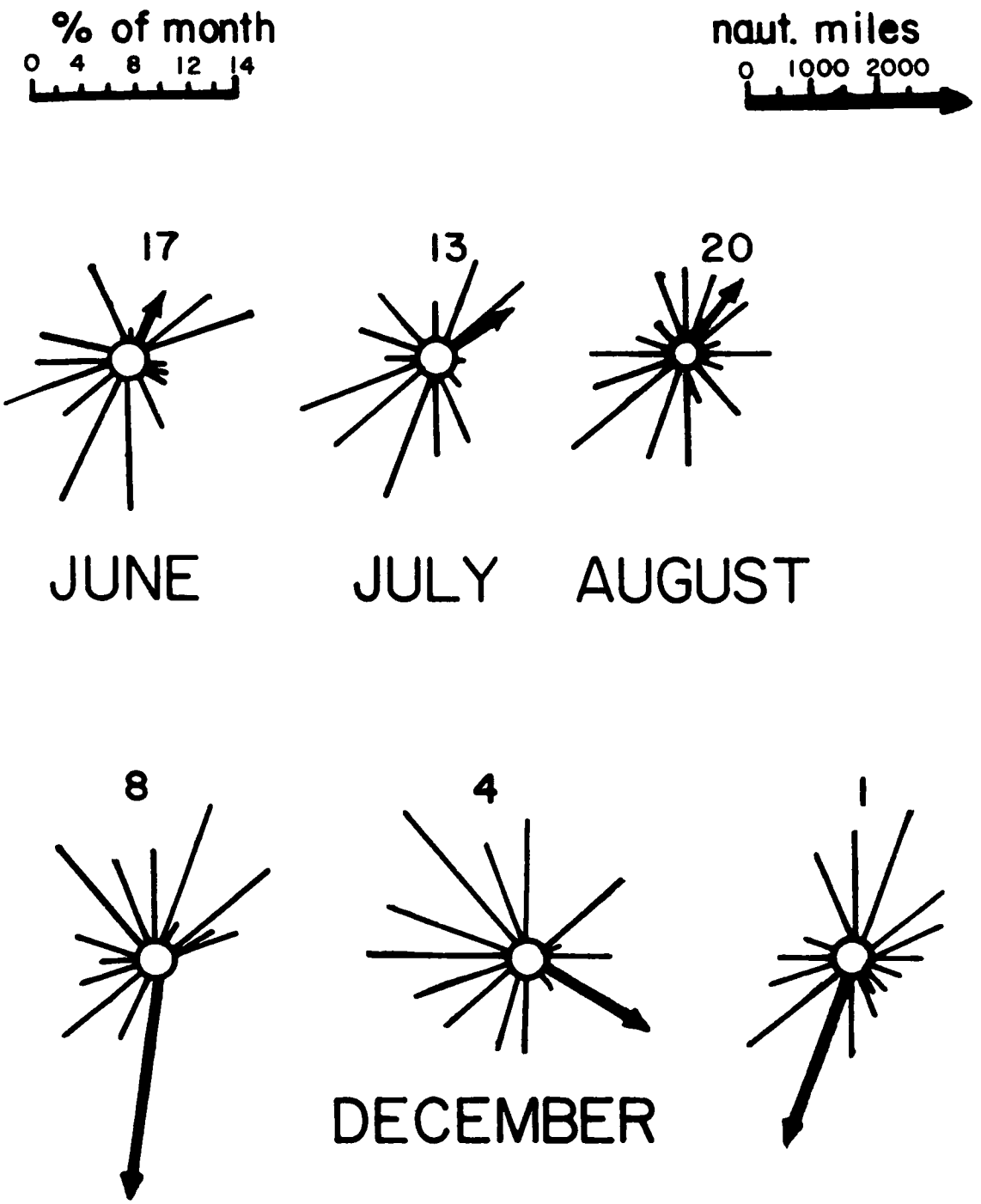
% of month
0 4 8 12 14
naut. miles
0 1000 2000
17
13
20
JUNE
JULY
AUGUST
8
4
1
DECEMBER
SEPTEMBER
FEBRUARY

Winter Conditions

Pronounced stratification of the shelf waters usually becomes obliterated in September (Harrison and others, 1967), due to chilling, increased wind stress, and a reduced river effluent.

Wind--Seasonal Changes

Summer

Based on U.S.C. & G.S. wind data (83rd Congress, 1953) and the average yearly wind rose (Fig. 26) the dominant direction of the wind in the summer is from the southwest and the velocities are moderate to light. The strong stratification of the water column affects the penetration of the moderate offshore winds. The strong density gradient impedes most of the influx of energy from the wind set-up current and generally the current direction of this upper layer is dominated by the wind direction. Thus "direction and rate of drift below the thermocline are influenced less directly by the wind. . ." and "the flow beneath the thermocline is, at times, entirely different than the surface drift" (Harrison and others, 1967).

Winter

North winds predominate during the winter season (Fig. 26) and are considerably stronger, with as much as 2.5 times the energy of any other direction (Neuman and James, 1955). These stronger winds affect a deeper segment of the unstratified water column and consequently are more influencial in development of both bottom and surface currents.

Salinity Driven Circulation

Harrison and others (1967) describe the salinity and circulation of the Chesapeake Bay, its function in the development of currents, and its effect on the water column of the Chesapeake Bight. They note:

> Chesapeake Bay is a relatively shallow coastal plain estuary where fresh water from land drainage is mixed with salt water from the sea by tidal action. The circulation in Chesapeake Bay, maintained by the passage of fresh water through the system, consists basically of a two-layered flow. The upper layer of less dense water has a net flow toward the sea and the denser more saline lower layer has a net flow toward the head of the estuary. The estuary, then, continuously receives ocean water, though in varying quantity depending upon river discharge. The maximum flow in the upper and lower layers occurs during periods of maximum river run-off and diminishes as the fresh water contribution lessens.

Therefore fluctuations in the effluent from the Bay will cause fluctuations in the water column stratification and bottom drift direction and magnitude.

Non-Tidal and Tidal Currents

The sea bed drifter and drift bottle data of Harrison and others (1967) within the Chesapeake Bight indicate interaction of river run-off, wind, and stratification of the water column in the production of non-tidal shelf drift currents. Previous authors have attempted to correlate the influence of the physical properties of temperature and salinity on surface waters (Miller, 1952) or the effect of estuarine effluent on the net bottom drift (Bumpus, 1965). Harrison and others (1967) described a permanent flow at the surface which was generally from north-to-south and known to be stronger from early fall to mid-spring than in the summer months when it may be absent or temporarily reversed. This correlates closely with Miller (1952) and his inferred near shore southerly "coastal drift". Howe (1962) has noted that this drift has been considered by Miller (1952) to be a counter-current to the northward flowing Gulf Stream. However, no specific mechanism for the creation or maintainence of this "permanent southerly drift" has been postulated in the literature. Howe (1962) suggests "the drift on the shelf will be influenced a great deal

by the varying wind effects, particularly during the winter months, when it is expected that the river run-off and temperature variations will be at a minimum, local density currents will tend to disappear, and thereby provide more suitable conditions for mass transport due to storms." Norcross and others (1962) observed that the greater part of the Chesapeake Bight is crossed by a "meandering but generally southerly drift having velocities of 10 to 14 miles per day."

Bottom drift, calculated from Harrison's work, maintained a pronounced trend toward shore to the southwest throughout all seasons (Fig. 16, 1967) except for a radius of 40 km about the mouth of Chesapeake Bay, where it trended bayward. Bumpus (1965) used sea bed drifters to determine a general "bottom residual current" flowing into all major estuaries of the Middle Atlantic Bight. He attributed these dominant shoreward bottom currents to be the consequence of a seaward flowing surface effluent from the estuaries consuming saline bottom water, and thus causing a compensatory landward flow on the bottom. Harrison observed a similar returning compensatory bottom drift toward Chesapeake Bay especially during periods of high river run-off and strong northwest winds which blow effluent out of the bay.

Haight (1942) in a comprehensive study of lightship current data determined the average velocity and type of surface tidal currents off the Mid-Atlantic coast. The data pertinent to the Chesapeake Bight was obtained from the Chesapeake Lightship, 19 km offshore. He determined the average ebb and flood tidal surface velocities to be .15 knots (8.3 cm/sec) with maxima in the east-west direction. He described the tide as a rotary tide with very light and variable velocities.

Harrison and Pore (1967) developed a group of theoretical

correlation models between wind or run-off and surface and bottom drift components. These models were based on vectors of surface and bottom drift inferred from drifter recovery data and correlations with winds and run-off by means of multiple linear regression procedures.

The components of the resultant drift vector of any given water particle were assigned $\bar{U}$ or $\bar{V}$ values. The $\bar{U}$ component approximates the positive east-to-west component of drift, and the $\bar{V}$ component approximates the positive north-to-south component of drift. Wind components were also represented by similar vector resolution into U, onshore and V, alongshore, components. A basic assumption in formulation of predictor equations was that surface current and wind direction were in close agreement. Harrison and Pore discuss fully the procedure and calculations used to derive their predictors. With a screening procedure, a small number of predictors were selected which contain nearly all the predictive information.

Schematic diagrams of the correlation of wind, river effluent, and surface and bottom currents were made with the information from the density stratification and number of days related drifters were en route. These diagrams (Plate IV, 1967) attempted to show the relationships of wind or run-off with the surface and bottom currents by means of correlation coefficients evaluating the closeness of fit the predictor equations matched the actual field measurements. However, these diagrams don't offer a very good explanation about what occurs in Chesapeake Bight and Harrison and Pore seem to lack a good explanation to resolve the discrepancies in correlation of the components. They did observe that multiple-predictor equations would be a more effective means of correlating the influence of both wind and run-off.

Figure 57. Swell diagram prepared by Corps of Engineers.

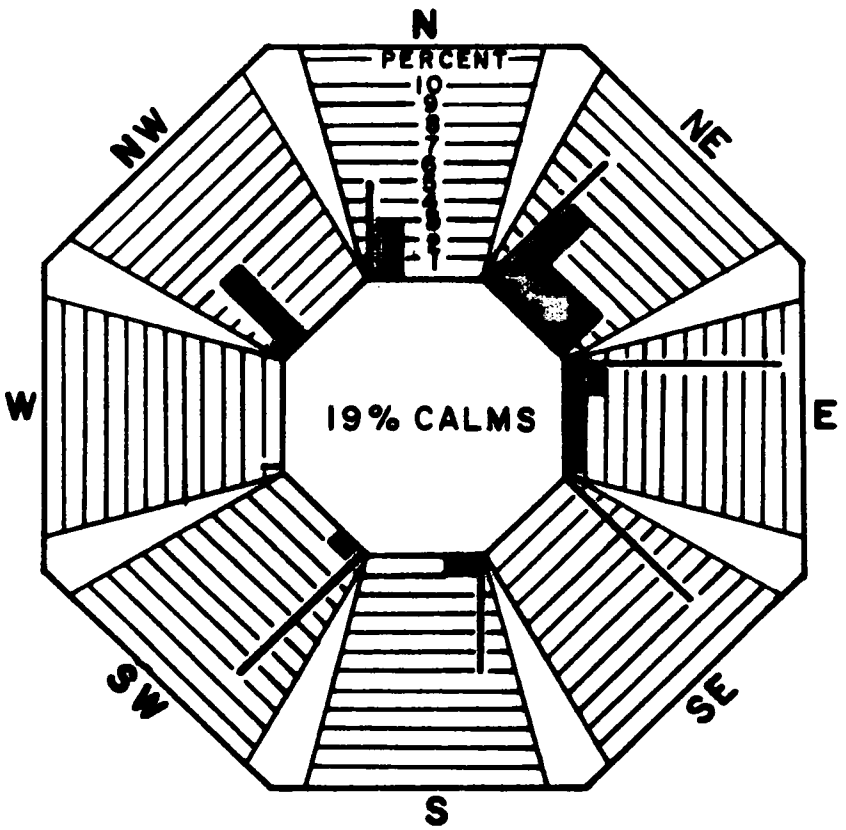

LOW SWELLS (1-6 FEET)

MEDIUM SWELLS (6-12 FEET)

HIGH SWELLS (OVER 12 FEET)

SWELL DIAGRAM
VIRGINIA BEACH, VIRGINIA

Figure 28. Percent of swell occurrence in the Chesapeake Bight. After Weinman.

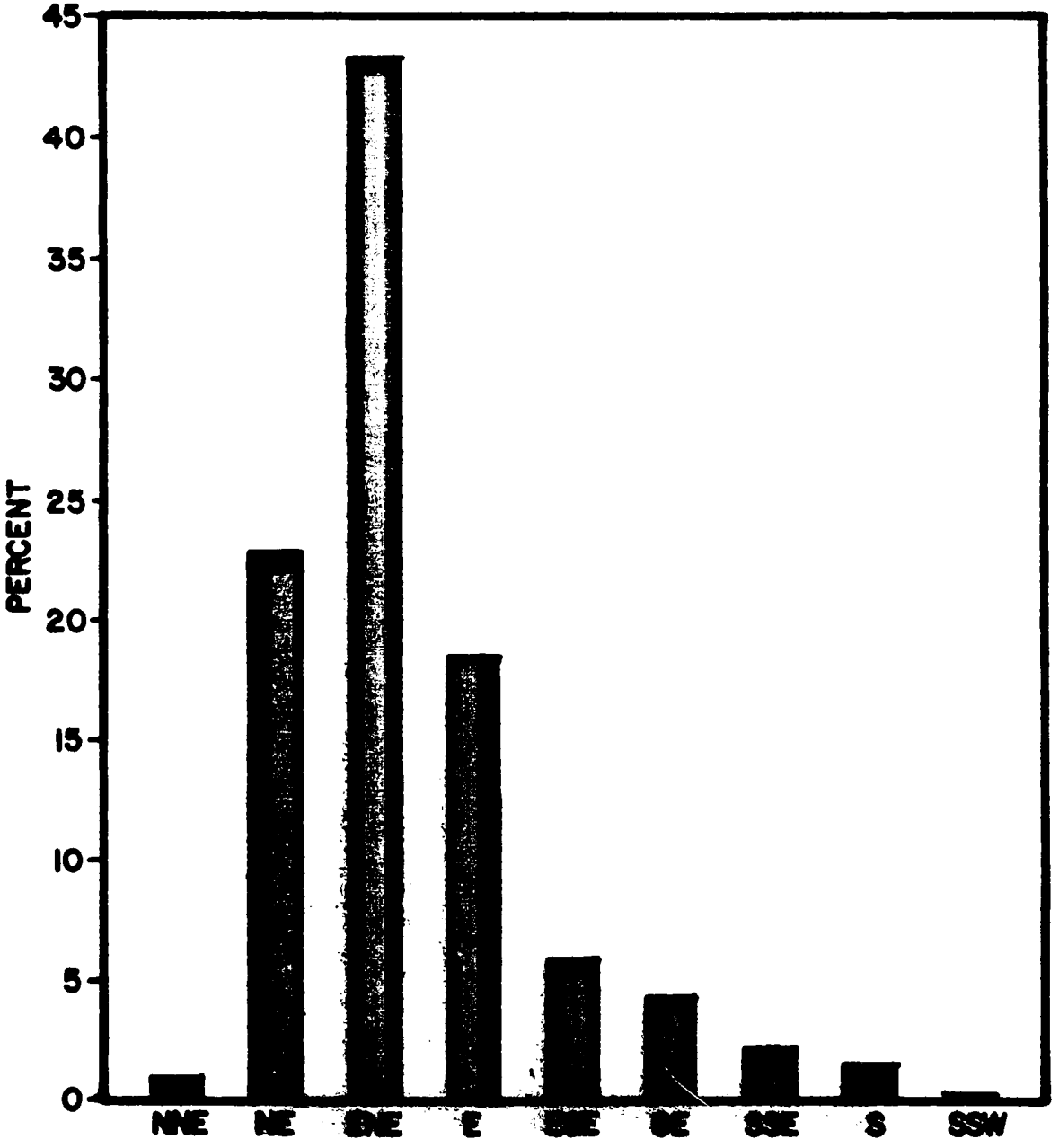
45
40
35
30
25
20
15
10
5
0
PERCENT
NNE
NE
ENE
E
ESE
SE
SSE
S
SSW

Wave Climate

Waves influence the currents of the Chesapeake Bight and their dominant directions vary with the seasons based on a similar variation of wind direction. A swell diagram (Fig. 27) illustrates the dominate wave trends and heights found off the Virginia coast.

The largest percentage of the swells move from the eastern quadrants and especially from the east-northeast (Fig. 28) (Weinman, unpublished Master's thesis). The greater percentage of the swells with low wave heights (1-6 feet) are from directions that would tend to produce northward drift. These low swells are most evident in the summer season when moderate offshore to southerly alongshore winds prevail. However, medium and heavy swells occur during a large percentage of the time from the northwest. These would tend to cause wave set-up near the shoreline resulting in a slight shift in a southward nearshore drift. These conditions occur most frequently during the winter months during periodic "northeaster" storms.

SHELF SAND RIDGES: A LITERATURE SURVEY

Before the hydraulic data can be discussed and related to the ridge and swale topography which underlies it, it will be necessary to review hypotheses presented in the literature concerning the genesis of current built submarine sand ridges. Sand ridges can be categorized according to the hydraulic mechanisms proposed for their deposition and maintenance, their morphology, and their observed position on the continental shelf. Two major categories are sand ridges on tide-dominated shelves and sand ridges on wave-dominated shelves. These can be further classified as straight versus sigmoidal, or as estuarine, beach tied, or isolated.

Tide-Built Ridges

The most striking ridge topographies are in tidal shelf seas. The earliest work on tidal ridges was done in the North Sea by Van Veen (1935). He noted that the southern North Sea "was found to possess a remarkable bottom of a wavelike structure. . . . The heights of these submarine sand dunes were often 10 meters or more." He suggested that alternating ebb and flood currents produced these structures. Houbolt (1969) described the ridge topography of the Southern Bight of the North Sea. He relates "within the Bight are 3 major areas of gently curved to elaborately sigmoidal, subparallel, sand ridges. . . . Crests and flanks tend to be of medium sand, while troughs contain lag deposits of coarse sand, pebbles and shells." He observed that the ridges are symmetrical to asymmetrical in cross-section. The latter are moving northeast, perpendicular to their long axis and the tidal currents, as a consequence of sand waves moving over the crests. Off (1963) discussed characteristic types of sand accumulation formed by tidal currents. The "tidal current ridges" appear

to be present wherever tidal current velocities range between 1 and 5 knots and are parallel to this current. He has noted that tidal ridges are found on a world wide scale at the heads of bays, at the mouths of large rivers, along tidal coastlines and even in the shallow open sea.

Allen (1968) proposes two categories of tidal current ridges based on the specific generating mechanism: (1) the sigmoidal type formed by ebb-flood current systems (Van Veen, 1935, Robinson, 1956, 1960), and (2) the rectilinear type ridges which seem to be more readily explained as a consequence of helical flow (Houbolt, 1968, Off, 1963, Allen, 1968).

Ebb-flood current systems were first described as a mechanism for producing shoals and tidal channels by Cornish (1901). Cornish noted that in English estuaries tidal flood flow took a direct, short-cut path towards the head of the estuary and in so doing moved up and over shoals and shallow flats. Ebb flow, on the other hand, tended to be somewhat more confined to the deeper, main meandering channels. Maximum flood and ebb flows even within the same channel tended to follow different, mutually evasive paths.

Ludwick (1970) attributed to ebb-flood channel flow the formation of the Chesapeake Bay mouth shoals and discussed the probable sediment transport mechanism of bed shear stress distribution associated with the net nontidal (residual) flow pattern. This residual flow has been discussed by Robinson (1966) and is the net difference in velocity and duration of the ebb and flood flow in a tidal cycle within each tidal channel. Though shallow sandy estuaries are the "type locality" for ebb-flood channel systems (Ludwick, 1970; Robinson, 1956, 1966), Van Veen has cited these systems within the Southern Bight of the North Sea.

Van Veen (1950) presented a detailed analysis of the concept,

explaining and defining paired ebb and flood channels, and illustrating characteristic patterns of ebb-flood channel systems, and describing circulating sand currents ("zandneer"). These occur when two parallel residual currents of the opposite sense (ebb versus flood) establish a shoal along their zone of shear. This shoal experiences sand transport in opposite directions on opposing sides of the ridge. Consequently, during periods of peak velocity of each flow small bedforms migrate away from the high velocity axis of the flow toward the crest at an angle to the ridge axis. Sand entrained in the stronger residual can actually spill over the crest to be picked up by the opposed residual flow on the other side. Thus the same sand particle could be trapped within the circulating cell during a finite residence period and be continuously carried around the shoal. This concept has been figured by Houbolt (1968) in his discussion of ebb-flood, asymmetric sand ridges.

Helical flow or spiral flow is a secondary transverse component of flow (Tanner, 1963) which is associated with a dominant, longitudinal component. The resultant flow pattern is helical. The helical flow of Houbolt (1968), Allen (1968) and Off (1963) are systems of spiralling cells flowing parallel to ridge axes. The troughs contain the descending flow, common to two adjacent half cells, with surface convergence and bottom divergence. The ascending limb of two adjacent half cells is centered over a ridge crest, with bottom convergence and surface divergence. Houbolt has suggested "that the tidal currents are stronger over the swales than over the ridges. To compensate for these differences in velocity the water will flow in two long spirals in such a way that the water over the bottom is directed outward from the swale towards the crest of the ridge." He observed that type of motion on some of these ridge systems and notes:

> The meeting of two masses of water with different current velocities and directions is usually revealed at the surface of the sea by current rips. Two types of current rip are observed. One type shows up as long foam lines and often contains concentrations of driftwood and other floating objects. Here the surface currents obviously converge. Such current rips were always found over the swales and never over the ridges. The other type of current rip only shows up as a difference in wave height and length and never shows a concentration of floating material. Such rips are explained as areas of diverging surface currents. They were frequently encountered over or near the crests of ridges.

Allen (1968) discussed a three-dimensional type of unstable motion which he considers to ordinarily be comprised of "an array of pairs of oppositely rotating helical spiral vortices whose axes lie parallel to flow. Allen offers a rule concerning the relationship of bedform configuration and the flow properties and states "when the motion is three dimensional, the longest dimensions of the bedforms generated are parallel to flow while the perturbations are transverse to the motion."

Smith (1969) discussed a sand ridge on the south coast of Cape Cod that he suggested is maintained by rotary tidal currents. He considers the origin of this sand ridge to be a small recessional moraine which underwent reworking due to wave action and tidal currents until a ridge was formed "in dynamic equilibrium with the tidal current system." Smith discussed a mechanism for the generation of longitudinal sand ridges. He suggests these ridges can grow if rotary tidal currents have their maxima parallel to the ridge. Thus the ridge will be at a small angle of attack to the flow through most of the high-velocity segment of the tidal cycle. The growth mechanism then reduces to a two-dimensional reversing cross-shoal flow driven by the "cross-shoal pressure gradient" and an upstream phase shift in the boundary shear stress maximum (Smith, 1969). He notes "flow in a natural channel is a shear flow, that is, a flow in which the velocity increases with distance from the bed. Boundary

shear stress will increase near the bed when such a flow moves over an upward-sloping bed as the higher velocity water will move closer to the bed due to its inertia. Consequently, the shear upstream from the crest of a sand ridge will be more and according to Smith will cause sand to be transported over the crest. Thus, the two flanks of a ridge will grow alternately, throughout a tidal cycle. Smith suggests that ideally this process of growth would continue until the crest reached the free surface but will not due to wind-wave diffusion. Thus the ridge height will be a response to "the rate of diffusion of material due to the wind-wave internal velocity field and the rate of growth of the ridge due to the basic flow" (Smith, 1969). Smith suggests this mechanism is a probable one for sand ridges in open tidal seas with rotary tidal currents. It should be noted that the three hydraulic mechanisms discussed are not mutually exclusive and are probably not the only mechanisms responsible for tidal ridge growth and development.

Ridges on Wave-Dominated Shelves

The shelf area of the Middle Atlantic Bight does not have strong tidal currents. Yet Shepard (1963) describes the Middle Atlantic Shelf as a broad sand plain characterized by a subdued ridge and swale topography "comparable to the barrier islands and their inner lagoons which extend along much of the present coast south of New York." Uchupi (1968) who has mapped and described this topography suggests the ridges are not relict, but instead are modern features forming during intense storms and remaining inactive between storms.

The distribution of Atlantic shelf ridges can be separated into offshore ridge and swale topography and nearshore ridge clusters which

tie to the beach. Swift (1969) notes that one of the most perplexing problems of the degree of adjustment of relict shelf surfaces to the modern hydraulic regime has been the origin of the ridge and swale topographies on these surfaces. A further problem of the shelf ridges is whether the offshore ridges and the nearshore beach-tied ridges are a related phenomenon. Sanders (1963) suggests that the main beach-tied ridge of the nearshore False Cape system is a drowned Pleistocene beach ridge. Yet Shepard (1963) has interpreted his ridges as a relict topography consisting of submerged barriers reflecting the littoral record of the Holocene transgression. The authors maintaining a relict origin for these ridges don't agree on which geologic period the ridges represent and their data for making these conclusions may not be sufficient for arriving at such an origin.

Moody (1964), in a detailed study of a nearshore ridge system off Bethany Beach, Delaware, has cast doubt on the relict interpretation. This ridge and swale topography consists of a group of fourteen parallel ridges trending obliquely to the shoreline. The ridge relief increases southward to a maximum of 7 meters and ridge asymmetry and length increases southward. Median grain size is finest on the southeast flanks of the ridges with a coarse maximum in the trough sediments.

Moody has compared bathymetric surveys from 1919 and 1961 and notes that ridge crests show a maximum movement of 250 meters toward the southeast. He believes that sand is moving southeast across the ridges in the direction of asymmetry and ridge movement. Moody observed the position of the ridges before and after the Ash Wednesday storm of 1962. He indicated that the ridges moved to the southeast during the storm a maximum of 70 meters. Thus, Moody suggests that the Bethany Beach ridge

system may be primarily a response to storm regimes. He speculates that the ridges may be generated in the nearshore zone, where some overtake others to form larger ridges. He further speculates that as sea level rises, these become quiescent large-scale hydraulic bedforms, occasionally activated by severe storms.

Swift and others (1970) have undertaken a study of the False Cape Ridge system. These ridges trend obliquely to the shoreline in a northeast direction. Second order ridges on the flanks of larger ones reveal a subdued asymmetry with steeper slopes facing away from major troughs and toward major crests (Fig.2). Topography and grain size vary sympathetically, with coarse-grained troughs, medium-grained crests, and fine-grained ridge flanks. Swift and others suggest that spiral flow channels and ebb and flood dominated channels might occur in response to the occasional storm surges of the Atlantic shelf, as well as in response to the strong tides of the North Sea.

Figure 29. Schematic diagram of summer conditions affecting bottom and surface currents. Large arrow from Chesapeake Bay indicates strong effluent flow.

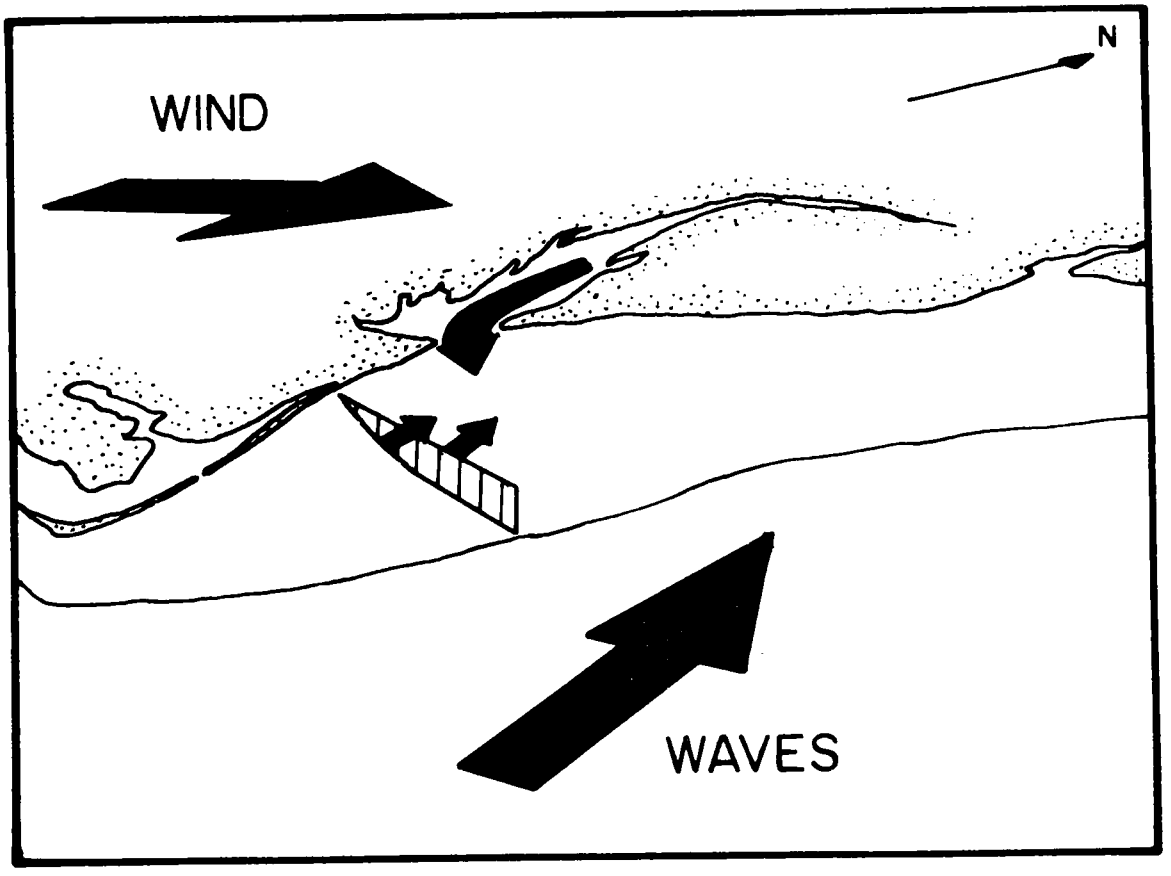
N
WIND
WAVES

INTERPRETATION OF DATA

Measurements of the currents found in the Chesapeake Bight have been mainly based on a lagrangian method of measurement utilizing "current followers" (Okubo, 1969) and the majority of the past studies dealt mainly with surface waters. The current measurements undertaken in this study utilize an Eulerian approach, whereby the velocity is monitored at one point on the bottom with an instrument package. The monitoring at various locations off False Cape was undertaken to determine if bottom drift could be resolved into genetic components, and to predict what effect this current regime has upon the bottom sediment and topography within the study area.

The False Cape ridge and swale topography seems to be a response to a two-fold hydraulic regime; a fair weather regime and a storm regime. These two ridges tend to affect the ridges in quite different ways and the combination of the two seem to be essential for the maintenance and development of such a topography.

Fair Weather Hydraulic Regime

Summer

Most of the monitoring stations were undertaken in fair weather during the summer or late spring; and, consequently, a more specific picture can be deduced for this season than for the winter regime. Based on the summer fair weather data a schematic diagram (Fig. 29) was constructed to show the relationship of the predominate offshore wind, the predominate wave direction from the southeast, and the effect of strong Bay effluent on the bottom and surface currents of the southern Virginia inner shelf waters. The diagram (Fig. 29) is based on computed bottom current residual directions for various stations (see Appendix I), observed

wind and wave directions, coupled with wind, wave and run-off data from the literature.

The northerly bottom residual current inferred in Figure 25 is probably a response to the strong effluent from Chesapeake Bay. The compensatory, bayward-flow of saline bottom water is characteristically stronger during the summer season. This northward bottom drift is able to respond better during the summer when the strong density stratification reduces the influence of wind drift. Southeast winds generally dominate the currents above the sharp thermocline causing a net northward surface drift.

The northerly bottom drift appears on the progressive vector diagrams of stations 2,3,4, and 6 (Fig. 21, 22, 23, 25). A northerly bottom residual of approximately 3.8 cm/sec seems to trend more towards the northwest at the outer station (6) than the more southerly inshore stations. The progressive vector diagram (Fig. 25) at first observation appears to be a response to a tidal component surimposed on a constant northward non-tidal drift. However, the changes in direction do not correspond with calculated changes in the tide. The number of hours represented by the three major segments are not equal to a tidal period. They may possibly represent large scale eddies associated with the tidal jet at the mouth of Chesapeake Bay.

The bottom current velocity is generally light with average speeds of 4 to 6 cm/sec (see Appendix I). Thus it can be inferred that during the relatively calm periods of the summer season the trough bottom currents will not have a large potential for transport of sand and the ridges will not experience noticeable movement or aggradation.

Fair Weather Degradation of Ridges by Waves

Effect of Maximum Orbital Velocities. Two fair weather monitoring stations were chosen for analysis of the role of fair weather wave surge in the maintainence of the ridges. These were station 3 on the crest of B ridge (Fig. 16) and station 5 on the crest of C ridge (Fig. 16). It can be seen from the rose diagrams (Fig. 16) and the progressive vector diagrams for these two stations (Fig. 22, 24) that the residual bottom current on the B ridge station seems to trend north with little variance. However, the pattern of bottom current direction of station 5 on the crest of C ridge shows a very diffuse direction pattern and suggests the influence of a weak rotary tide with westerly residual component.

There are various factors which must be considered in analyzing the current direction. The major consideration is the depth of water of the two crests. B ridge crest is in approximately 8 meters of water and C ridge crest is at a depth of 13.5 meters. No sharp density gradient was observed on B ridge, yet on C ridge, divers noted a very pronounced thermocline at about 6 meters. According to Harrison and others (1967, p. 5) such a strong density gradient can reduce the influx of momentum of wave energy. Thus the shoaler station 3 experiencing more mixing probably is more influenced by wind effects than station 5. During their respective periods of observations (Appendix I), B ridge experienced a dominant southeast swell with .5 to 1 m wave heights and C ridge was only affected by a less than .5 m swell from the southeast. With this information and the bottom current measurements of each station, an analysis of the effect of sediment transport by the oscillatory motion of the waves was undertaken.

It should be possible to calculate the theoretical threshold of

grain movement for a given monitoring station from the measured modal diameter at the station, and compare this with the velocities recorded at the station. However, according to some authorities threshold velocities are nearly independent of grain size for diameters smaller then 0 phi (McQuivey and Keefer, 1969, Fig. 1). Cook (1969) has noted that many problems arise in attempting to measure and quantify an initial grain transport velocity. He calculated threshold velocities for all grain sizes and observed they were practically identical values. He also noted that oscillation ripple marks segregate sediment by size with the extremes located at the crests and troughs. Thus, the "ripple marks create a spectrum of energy niches so that particles of different hydraulic size may be at equilibrium at the same bottom location.

Mechanical problems within the monitoring system and data reduction also affect the determination of threshold values. The actual measured bottom velocities never exceeded 10 cm/sec, and according to Cook's (1969) observations, particle motion does not commence until the current is at least flowing at 18 to 21 cm/sec. However, the true peak velocities probably greatly exceeded 10 cm/sec. The lack of stronger velocities is believed to be a function of the integration circuitry of the readout meters when time constant 2 is used. Instantaneous peak currents are averaged out and the record shows only a smoothed velocity oscillation. Observations have been made in time constant 1. In this mode, peak velocities readily peg the meters and values of 30 to 40 cm/sec are common. However, the recording system used was not able to change scale to utilize such a record and the current meter system had to operate in time constant 2. As a result of these difficulties, no attempt to directly relate surge velocities to sediment threshold velocities was

Figure 30. Peak velocity progressive vector diagram and rose of Station 5 in crest of C ridge. Net residual is 1.1 cm/sec towards the west-northwest (278°).

N
end

Figure 31. Peak velocity progressive vector diagram and rose of Station 3 on crest of B ridge. Net residual is 2.7 cm/sec towards the northwest (324°).

N
end

made. The analysis of the most intense third of the instantaneous velocity samples of each station is not an attempt at quantitative analysis of the complex velocity structure of an oscillatory motion near the bed, but is , instead, intended as a qualitative means of predicting the probable movement of sand due to the maximum orbital velocities during the fair weather hydraulic regime.

The plot of peak velocity vectors from C ridge (Fig. 30) nearly mirrors the initial progressive vector diagram and suggests that transport associated with maximum orbital velocity was in the same direction as the residual bottom currents measured with a net velocity of 1.1 cm/sec. This ridge crest is probably not undergoing significant oscillatory sand transport under the light winds and wave conditions of the monitoring period.

The vectors of peak velocity plotted for the B ridge crest station (Fig. 31) show a significant shift in the direction of residual bottom motion from the total velocity progressive vector diagram (Fig. 21). This peak velocity residual seems to reflect the affect of the dominant southeast swell with sediment transport across the ridge, while the total bottom current appears to be moving in a northwest direction along the crest. Thus, the average velocity residual of Figure 21 probably does not reflect the transport direction of coarser sand.

If it is assumed that only these peak velocities are greater than or equal to the calculated velocity for the threshold of grain movement, then the peak velocity vector diagram suggests that sand is being transported off the crests onto the landward flank of B ridge by asymmetric wave surge and that the effect of fair weather wave surge is to flatten the crest of the ridge.

Scuba Dives to Ridge Crests. Evidence to support these calculations

Figure 32. Photo of an oscillation ripple being measured with a modified Newton ripple meter.

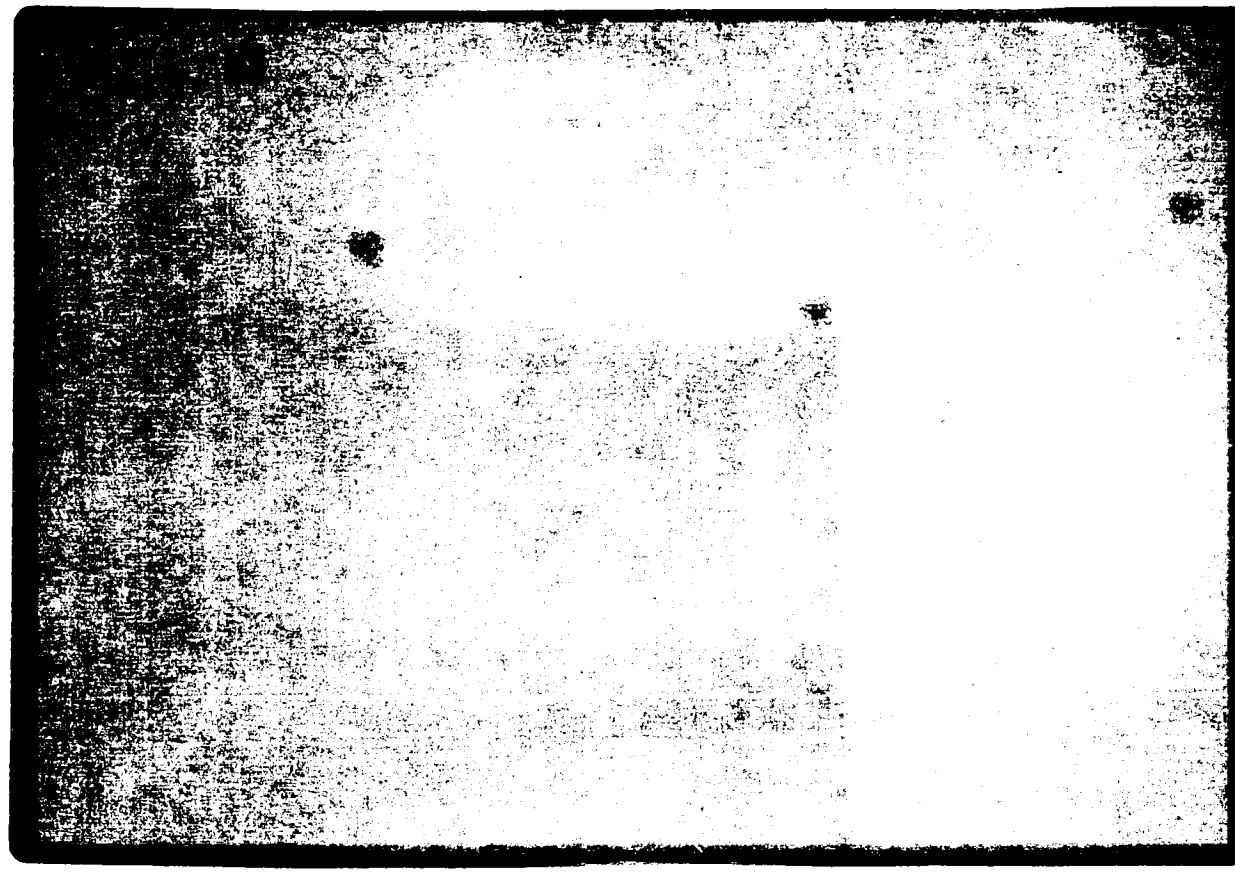

was obtained from scuba dives on the B ridge crest and other ridge crests in the study area. Observations of medium- to coarse-grained, short-crested, oscillation ripples actively migrating under the influence of wave surge have been made (Fig. 32). Ripples were observed passing over the current meter frame and over shells on the bottom. Cook (1969) observed no significant movement of ripples, in spite of surge inequities and net transportation of bottom sediment. Newton (1968) states, to the contrary, that symmetrical ripples migrate and that net sand transport within a ripple field can be unrelated to ripple migration. Scott (1954) observed ripple migration in a flume experiment at various wave steepnesses and depth ratios.

The presence of ripples and the observed sand transport indicate surge velocities strong enough and frequent enouth to transport and degrade the ridge crests in the shallow water areas.

Grain Size Evidence of Crestal Winnowing by Waves. Swift and others (in press) have sampled the False Cape Ridges and determined the grain size distribution. We observed medium-grained, well-sorted sands on the crests and suggest these were swept up onto the crest during storms and subsequently winnowed by fair weather swells. This crestal lag is finer and better sorted than the primary lag of the trough but not as fine and well-sorted as the very fine flank deposits, which have been winnowed out of the crests by the waves.

The seaward flanks are finer-grained than the landward flanks. This phenomenon may be explained by the observations of Keulegan (1948) who studied sand transport on a rippled bed in shallow water. Coarser sand is transported as bed load in a shoreward direction as the low swell crest passes over. However, the finer sand becomes entrapped in small

Figure 33. Schematic diagram of winter conditions affecting bottom and surface currents. Small arrow from Chesapeake Bay represents reduced effluent.

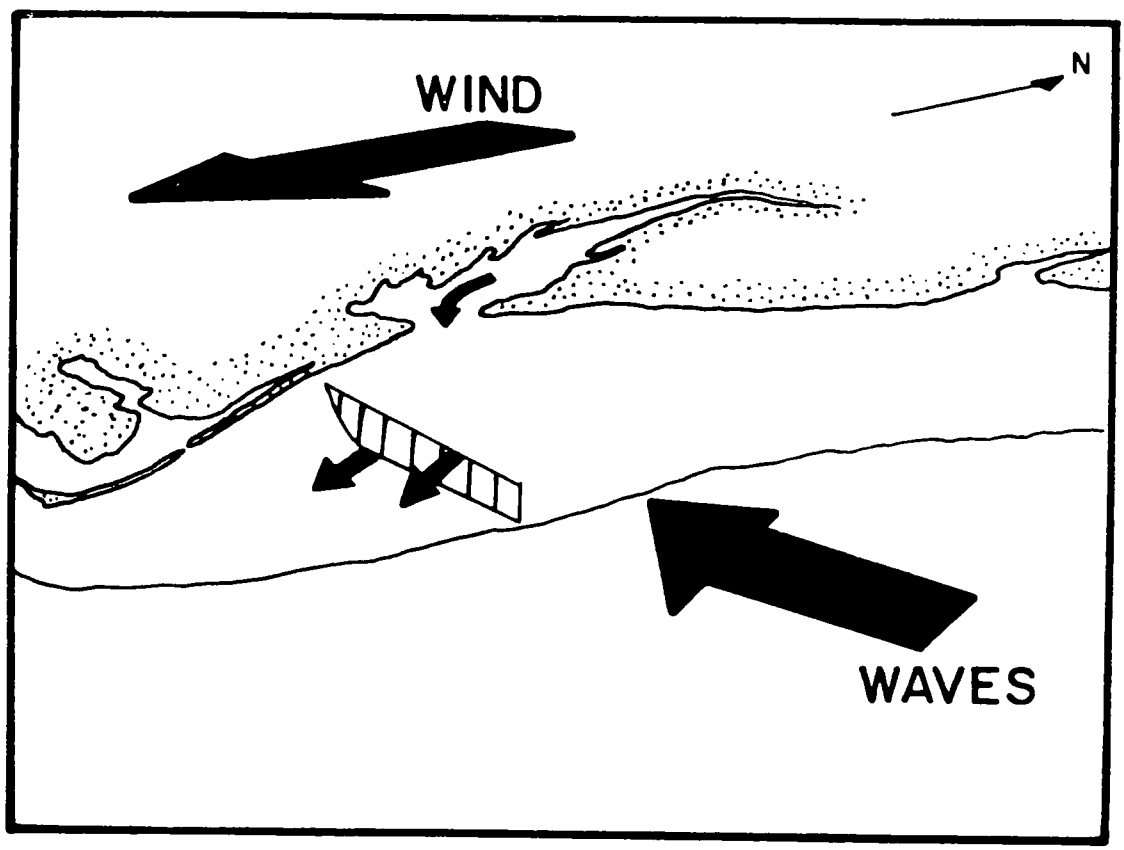
WIND
N
WAVES

eddies within the ripple troughs and becomes suspended. The suspended finer sand is then transported seaward as the trough of the wave moves over the ripple and the oscillatory water motion reverses. Thus finer, well-sorted sand on ridge crests may be transported off the crests onto the seaward flanks.

Winter

Evidence from Harrison and others (1967) and previous work mentioned in an earlier section suggests that the winter shelf experiences a general reversal in both bottom currents and surface drift (Fig. 33). This reversal is primarily due to the obliteration of vertical stratification of the water column allowing the influx of momentum of the stronger northerly wind drift currents to extend deeper. This drift is opposite in effect from the "Ekman drift" which is characterized by the dextral deflection of the current with respect to the wind direction. As these dominant north to northeast winds pile water against the coast, the geometry of the shoreline in the Chesapeake Bight causes this water to move southward, establishing a unique inner shelf drift. Coupled with wind effect is a marked reduction in the effluent from Chesapeake Bay reducing the bayward flow of bottom water. No monitoring stations were made during the winter months to determine the velocities of characteristic fair weather winter bottom currents. However, from wind and wave information, periods of calm and light winds are not as frequent during this period and bottom currents are probably not as weak.

Figure 34. A ridge during a northeaster. Waves breaking on ridge in upper right hand corner. Photo by McHone.

Storm Hydraulic Regime

The most frequent storms in the False Cape Area are "northeasters". Most mid-latitude cyclones ("northeasters") move across Georgia from the Gulf and up the Atlantic seaboard. Most hurricanes in this region also move north up the Atlantic seaboard. Since the storm centers are usually seaward of the shoreline, the nearshore areas experience the strong north and east winds of these counterclockwise wind systems. During a northeaster great masses of water are moved southward due to wave set-up pushing so much water towards the beach that it eventually veers and moves parallel to shore. Harrison and others (1967, p. 72) suggested that when the onshore component of the wind increased over the shelf in the northern part of the Middle Atlantic Bight, a net southerly drift (permanent flow) may be produced due to set-up on the southwesterly trending coast. If the storm center passes very close, then the inverted barometer effect is felt, and an upward bulge of the sea beneath the low pressure center will occur. The storm surge, or combined result of set-up and the inverted barometer effect can move along the shelf like an astronomical tidal wave, and like the latter, has an ebb and flood associated with it.

Station 1 in A trough (Fig. 16) was monitored during a relatively mild northeaster and is the only storm data available. The monitoring began under relatively calm conditions and the current appears to be a response to a nearly reversing tide and light wave action (Fig. 20). The northeaster developed rather quickly with 1.5 to 1.8 meter seas from the northeast. The progressive vector diagram (Fig. 20) shows a pronounced increase in current velocity and a prevalent southeast current direction. During this period waves were observed breaking on A ridge (Fig. 34). Water pumped over A crest by this surf must have caused a

Figure 35. Schematic diagram of observed storm currents (A) on A ridge and the hypothesized fair weather currents (B).

A

BOTTOM CURRENT →
SURFACE CURRENT --→
CREST – – –

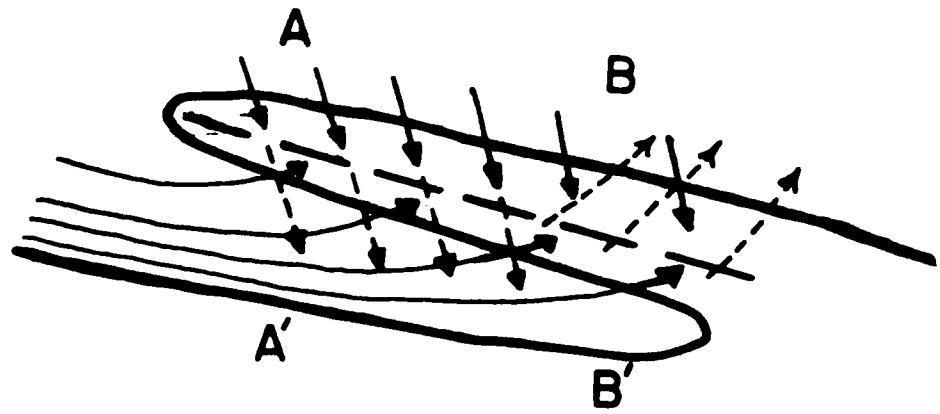

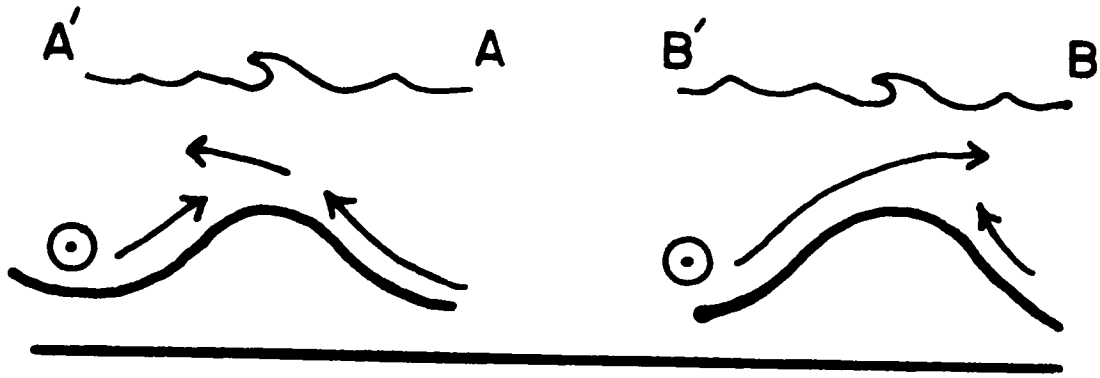

B

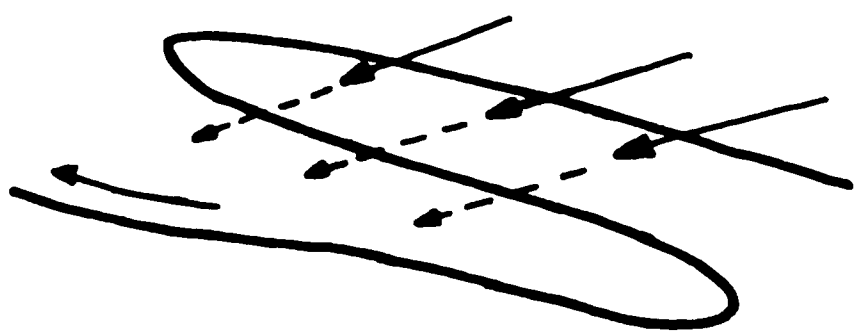

local intensification of the south trending wind set-up current. The wind and wave induced hydraulic head over A trough found relief by a sort of large scale rip current flowing diagonally seaward over the landward end of A ridge. Sea birds were observed to be convening at the landward head of the A trough, suggesting they were hunting fish that were being swept over the shoal crest of the ridge. Thus the shoreward and southern portion of A ridge crest was experiencing a seaward current toward the southeast while its northern and seaward portion was experiencing a shoreward bottom current (see Figure 35). Consequently, sediment was probably being transported from both sides toward the crest, with net landward transport over the northern end of the crest, and net seaward transport over the southern end. If there is northerly transport of sediment by wave drift currents on the seaward flank and over the crest of A ridge during periods of southerly swells (see Figure 35), then A ridge would constitute a circulating sand cell.

The observations and measurements were made in a northeaster of mild proportions as would be expected during the summer season. The currents generated by such a storm are usually damped out after, at the most, 3 or 4 days. However, these storms are usually prolonged during the winter season and several may pass in rapid succession so that southerly wave set-up currents may prevail for as much as 10 or 11 days. The winter intensification of wind and wave set-up is coupled with the lack of strong stratification allowing deeper transfer of momentum of wave drift currents. Hence, it seems probable that the bulk of sediment transport is accomplished during this season.

The effect of a strong northeaster was observed in 17 meters of water near the crest of "Z" ridge in May of 1971, two months after a very

intense March northeaster that approached the magnitude of the Great Ash Wednesday Storm of 1962. Observations were made of large, rounded, coarse-grained sand waves with heights of approximately 1.8 to 2.4 meters and wavelengths of approximately 9 to 12 meters. Fair weather oscillation ripples with heights of 6 to 10 cm mantled the sand waves. Infrequently sand was observed being transported near the crest of the sand waves. Troughs appeared to be stagnant with concentrations of fine fecal pellets and algae. Avalanche slopes were no longer present. Thus, it appears the sand waves are going through a period of degradation during the fair weather regime. They are now rounded but were probably asymmetric sand waves formed during the intense March storm.

Inner and Outer Ridges

It seems appropriate to divide the False Cape Ridge system into an inner group of A and B ridges and an outer group of C and Z ridges, on the basis of a limiting crestal depth of 10 m. The division seems significant in that it acknowledges a morphological difference; the inner ridges attach to the shore face, while the outer ridges are isolated. The inner more shallow ridges appear to be more frequently aggraded by storms and the observations show that they are sufficiently shoal to experience significant degradation during fair weather. A ridge, in particular, appears to be active much of the time, due to a complex interaction of wave drift and wind and wave set-up currents. If the ridges form an evolutionary sequence, then A ridge is probably undergoing active formation, while the outer ridges are perhaps merely being maintained by spiral flow cells associated with the strong southerly storm surge currents of winter.

CONCLUSIONS

The current meter monitoring stations have revealed information about the fair weather hydraulic regime in the summer season. One station recorded the effects of a moderate northeaster. The fair weather bottom current regime appears to be a response to the wind and wave directions and river run-off from the Chesapeake Bay as well as to the topography of the study area. The shallow inner ridge crests (A and B ridge) appear to be undergoing continuous degradation by the asymmetric oscillatory bottom current of the dominant summer swell, and fine sand is being transported off the crests onto the flanks and troughs. The finest sand may be moving seaward as a consequence of the sort of ripple fractionation described by Scott (1954). The outer ridges (C and Z ridge) appear to experience less effect from wave surge near the bottom and are probably quiescent until an intensification of swell height or storm surge currents occur. These stations are probably more affected by the strong stratification of the summer water column, reducing the penetration of wave energy. However, the deeper stations do reveal definite northerly residual currents suggesting a response to the compensatory bottom water flowing into the Bay.

Storms appear to be the major force in maintaining and building the ridges. The inner ridges apparently experience frequent rebuilding by south-trending storm currents experiencing spiral flow. Valuable information was obtained from the current record of the nearshore station monitored during the northeaster, pertaining to the southeast deflection of bottom currents influenced by wave set-up, and the effects of high waves breaking on shallow ridge crests were observed. This information and observations of probable storm surge sand waves on "Z" ridge suggest that

the storm hydraulic regime can affect even the deep outer ridges if the storm is intense enough.

The monitoring fell short of completely determining the year round components of the bottom currents within the study area. Due to boat malfunctions and rough weather the current monitoring was generally restricted to the fair weather regime. Some of the calculations, such as the peak-velocity calculations required assumptions that could be obviated with modifications to the equipment. Repetition of stations at similar times of the year would strengthen the observations made from just one station in one twenty-four hour period.

Suggestions for further work include hourly measurements of temperature and salinity to have better control of the water column stratification effect, hourly measurements of the velocity through the water column, measurements of the peak velocities at each monitoring period (every 30 minutes), and possibly bed load transport monitoring to correlate with peak velocity and compare the calculations.

REFERENCES CITED

Allen, J. R. L., 1968. Current Ripples. North Holland Publishing Co., Amsterdam, 433p.

Allen, J. R. L., 1968. The nature and origin of bedforms hierarchies: Sedimentology, 10: 161-182.

Bumpus, D. F., 1957. Oceanographic Observations, 1956, East Coast of the United States. U. S. Fish and Wildlife Service Special Scientific Report--No. 233, p. 1-132.

Bumpus, D. F., 1965. Residual drift along the bottom on the continental shelf in the middle atlantic bight area. Limnology and Oceanography, Supplement to volume 3, 48-53.

Burger, J. A., Klein, G. de V., and Sanders, J. E., 1969. A field technique for making epoxy relief-peels in sandy sediments saturated with salt water. J. Sed. Pet. 39: 338-341.

Caster, W. A., 1969. Near Bottom Currents in Monterey Submarine Canyon and on the Adjacent Shelf. Naval Post Graduate School, Masters Thesis (unpublished), 201p.

Cook, D. D., 1969. Sand Transport by Shoaling Waves. Thesis, University Southern California, 148p. (unpublished).

Cornish, V., 1901. On sandwaves in tidal currents. Geographical Journal, 18: 170-201.

Fisher, 1967. Development Pattern of Relict Beach Ridges, Outer Banks Barrier Chain, North Carolina. Thesis, University North Carolina, Chapel Hill, 250p. (unpublished).

Haight, F. J., 1942. Coastal Currents Along the Atlantic Coast of the United States. U. S. Coast and Geodetic Survey Special Publication, No. 230, 26p.

Harrison, W., Norcross, J. J., Pore, N. A., and Stanley, E. M., 1967. Circulation of shelf waters off the chesapeake bight. Environ. Sci. Serv. Admin. Prof. paper 3, 82p.

Houbolt, J. J. H. C., 1968. Recent sediment in the southern bight of the north sea. Geologie en Mijnbouw, 47: 245-273.

Howe, M. R., 1962. "Some direct measurements of the non-tidal drift on the Continental Shelf between Cape Cod and Cape Hatteras. Deep-Sea Research, 9: 445-455.

Hoyt, J. H., 1967. Barrier island formation. Geol. Soc. Amer. Bull. 78: 1125-1136.

Joseph, E. B., Massmann, W. H. and Norcross, J. J., 1960. Investigation of inner continental shelf waters off lower chesapeake bay, Part I--General introduction and hydrography. Chesapeake Science, 1: 155-167.

Keulegan, G. H., 1948. An Experimental Study of Submarine Sand Bars. U. S. Corps of Engineers Beach Erosion Board, T. M. #3, 40p.

Krumbein, W. C., 1939. Preferred orientation of pebbles in sedimentary deposits. Jour. of Geol. 47, No. 7: 673-706.

Ludwick, J. C., 1970. Sand waves and tidal channels in the entrance to Chesapeake Bay. Virginia J. Science, 21: 178-184.

McQuivey, R. S. and Keefer, T. N., 1969. The relation of turbulence to deposition of magnetite over ripples. U. S. Geol. Survey, Prof. Paper 650-D: D244-D247.

Miller, A. R., 1952. A pattern of surface coastal circulation inferred from surface salinity--temperature data and drift-bottle recoveries. Woods Hold Oceanographic Institution Reference No. 52-28, 1-14.

Moody, D. W., 1964. Coastal Morphology and Procession Relation to the Development of Submarine Sand Ridges off Bethany Beach, Delaware. The Johns Hopkins University, Ph.D. thesis (unpublished), 167p.

Neuman, G. and James, H., 1955. North Atlantic Coast Wave Statistics Hindcast by the Wave Spectrum Method. U. S. Corps of Engineers, Beach Erosion Board, Tech. Mem. No. 57.

Newton, R. S., 1968. Internal structure of wave-formed ripple marks in the nearshore zone. Sedimentology, 11: 275-292.

Norcross, J. J., Massmann, W. H. and Joseph, E. B., 1962. Data on Coastal Currents off Chesapeake Bay. Virginia Institute of Marine Science Special Report No. 31, p. 1-25.

Off, T., 1963. Rhythmic linear sand bodies caused by tidal currents, Amer. Assoc. Pet. Geol. 47 (2): 324-341.

Okubo, A., 1969. A note on the effect of dispersion on mean current measurements. The Johns Hopkins University, Chesapeake Bay Institute, Tech. Rept. 55, 20p.

Payne, L. H., 1970. Sediments and Morphology of the Continental Shelf off Southeastern Virginia. M. S. Thesis, Columbia University, 70p. (unpublished).

Pierce, J. W. and Colquhoun, D. J., 1970. Configuration of holocene primary barrier chain, outer banks, North Carolina. Southeastern Geology, 11: 231-236.

Pincus, H. J., 1956. Some vector and arithmetic operations on two-

dimensional orientation variates, with applications to geological data. Jour. of Geol., 74 (6): 533-557.

Robinson, A. H. W., 1956. The submarine morphology of certain port approach channel systems. Jour. Inst. Navigation, 9: 20-46.

Robinson, A. H. W., 1960. Ebb-flood channel systems in sandy bays and estuaries. Geography, 45: 183-199.

Robinson, A. H. W., 1966. Residual currents in relationship to shoreline evolution. Marine Geol., 4: 57-84.

Sanders, J. E., 1963. North-south trending submarine ridge composed of coarse sand off False Cape, Virginia (Abs.). Am. Assoc. Petrol. Geol. Bull. 46: 278.

Sanford, R. B. and Swift, D. J. P., in press. Comparison of seiving and settling techniques for size analysis, using a Benthos Rapid Sediment Analyzer. Sedimentology.

Scott, T., 1954. Sand Movement by Waves. U. S. Corps of Engineers, Beach Erosion Board, T. M. 48, 36p.

Shepard, F. P., 1963. Submarine Geology. Harper and Row, New York, 567p.

Shideler, G., Swift, D. J. P., Johnson, G. and Holliday, B., in press. A proposed standard section for late quaternary stratigraphy of the inner Virginia Continental Shelf. Geol. Soc. Amer. Bull.

Smith, J. D., 1969. Geomorphology of a sand ridge. J. Geol. 77: 39-55.

Swift, D. J. P., 1969. Inner shelf sedimentation: processes and products. In: D. J. Stanely (Ed.), The New Concepts of Continental Margin Sedimentation, Amer. Geol. Institute, Wash. p. DS-4-1 to DS-4-46.

Swift, D. J. P., Shideler, G. L., Avignone, N. F., and Holliday, B. W., 1970. Holocene transgressive sand sheet of the middle Atlantic bight--a model for generation by shore face erosion Discussion paper : Geol. Soc. Amer. Abst. 2 (7): 757-759.

Swift, D. J. P., Holliday, B. W., Avignone, N. F., and Shideler, G. L., in press. Anatomy of a shore-face ridge system, False Cape Virginia. Marine Geology.

Tanner, W. F., 1963. Spiral motion, sediment transport, and river development. unpublished paper presented at Federal Inter-Agency Sedimentary Conference, 12p.

Uchupi, E., 1968. The Atlantic continental shelf and slope of the United States: Physiography. U. S. Geol. Surv. Prof. Paper 529-C, 30p.

U. S. Congress, 83rd 1st session, 1953. Virginia Beach, Virginia, Beach Erosion Control Study. House Document 136, 45p.

Van Veen, J., 1935. Onderzockingen in de Hoofden in Verband mit de gesteheid der Nederlandse Kust. Neiuwe Verhandelingen Van het Bataafsch Genootschap Voor Proefondervindelikje wigs begurte to Rotterdam. Tweede Reeks, elfde deel.

Van Veen, J., 1950. Eb-en Vloedschaar systemen in de Nederlandse getijwateren: Tydschr. Koninkl. Ned. Aardrijkskundig Genootschap, 67: 303-335.

Weinman, Z., 19[illegible]. Analysis of Littoral Transport by Wave Energy: Cape Henry, Virginia to the Virginia--North Carolina Border. M. S. Thesis, Old Dominion University, (unpublished).

APPENDIX

Station Number	Date	Ship
1	10,11 September 1970	R/V ALBATROSS

Number of Readings	Number of Hours	Weather
56	28	Wind SW 15/ NE 25 Sky Fair / Cloudy (Northeaster)

Depth (m)	Swell	Period	Chop
9.8	.3m	9-11 sec	.3 S 1.5-2.0m NE

Bottom Currents (cm/sec)	Bottom Character
max 18 min 2.1 mean 5.7 residual 2.6, 130°	coarse sand ripples

Ripple Height	Ripple Wave Length	Crestal Continuity	Azimuthal Direction
7-10 cm	17-32 cm	———	NE-SW

Monitoring Systems Used
Bendix Current Meter Hydroproducts Wave Gage

APPENDIX I. Description of Monitoring Stations

Station Number	Date	Ship
2	8,9 June, 1970	R/V ALBATROSS

Number of Readings	Number of Hours	Weather
55	20	Wind ESE 10-15 Sky clear, mild

Depth (m)	Swell	Period	Chop
12.8	SE(145) .3m	9-12 sec	ESE .3m

Bottom Currents (cm/sec)	Bottom Character
max 6.7 min 2.1 mean 4.1 residual 3.6, 345°	rippled, coarse shelly sand

Ripple Height	Ripple Wave Length	Crestal Continuity	Azimuthal Direction
4-6 cm	19-27 cm	58-97 cm	E-W

Monitoring Systems Used
Bendix Current Meter System

APPENDIX I. Description of Monitoring Stations

Station Number	Date	Ship
3	18,19 June 1970	R/V ALBATROSS

Number of Readings	Number of Hours	Weather
52	26	Wind SW 15 Sky clear, fair warm

Depth (m)	Swell	Period	Chop
8	SW .6 m	7-11 sec	light

Bottom Currents (cm/sec)	Bottom Character
max 7.2 min 2.1 mean 4.1 residual 3.6, 010°	coarse sand 10% shell ripples

Ripple Height	Ripple Wave Length	Crestal Continuity	Azimuthal Direction
10-18 cm	39-50 cm	188-200 cm	SE - NW

Monitoring Systems Used
Bendix Current Meters Bedload bottles

APPENDIX I. Description of Monitoring Stations

Station Number	Date	Ship
4	15-16 July 1970	RANGE RECOVERER

Number of Readings	Number of Hours	Weather
28	14	Wind SE, Light Sky clear, fair

Depth (m)	Swell	Period	Chop
18.4	ESE .3 m	9 - 12 sec	SE .2m

Bottom Currents (cm/sec)	Bottom Character
max 7.7 min 1.5 mean 4.1 residual 3.6, 359°	mud on anchor no dives made

Ripple Height	Ripple Wave Length	Crestal Continuity	Azimuthal Direction
—	—	—	—

Monitoring Systems Used

Bendix Current Meters
Bedload Sampler

APPENDIX I. Description of Monitoring Stations

Station Number	Date	Ship
5	14,15 July,1970	RANGE RECOVERER

Number of Readings	Number of Hours	Weather
54	27	Wind SE, light Sky clear

Depth (m)	Swell	Period	Chop
13	ESE .3 m	9 - 12 sec	ESE .2 m

Bottom Currents (cm/sec)	Bottom Character
max 5.2 min 1.5 mean 2.6 residual 1.0, 264°	coarse shelly sand ripples

Ripple Height	Ripple Wave Length	Crestal Continuity	Azimuthal Direction
4-6 cm	12-17 cm	150-200 cm	—

Monitoring Systems Used
Bendix Current Meters Bedload Sampler

APPENDIX I. Description of Monitoring Stations

Station Number	Date	Ship
6	4,5 May, 1971	RANGE RECOVERER

Number of Readings	Number of Hours	Weather
47	24	Wind SW 15 Sky partly cloudy

Depth (m)	Swell	Period	Chop
21.5	ENE .3 m	8-11 sec	SW .3 m

Bottom Currents (cm/sec)	Bottom Character
max 14 min 1.2 mean 5.2 residual 3.6, 347°	medium sand no ripples

Ripple Height	Ripple Wave Length	Crestal Continuity	Azimuthal Direction
—	—	—	—

Monitoring Systems Used
Bendix Current Meters